Construction and Building Materials 260 (2020) 119788

Contents lists available at ScienceDirect

Construction and Building Materials

journal homepage: www.elsevier.com/locate/conbuildmat

Review

A review on alkali-activated binders: Materials composition and fresh properties of concrete

Md Manjur A. Elahi [a,*], Md. Maruf Hossain [b,*], Md Rezaul Karim [c], Muhammad Fauzi Mohd Zain [d], Christopher Shearer [e]

[a] Project Engineer, Construction Services Department, Intertek USA, Inc, Houston, TX, United States
[b] Faculty of Engineering and Built Environment, The University of Newcastle, Callaghan, Australia
[c] Department of Civil Engineering, Dhaka University of Engineering & Technology, Gazipur, Bangladesh
[d] Faculty of Engineering and Built Environment, University Kebangsaan Malaysia (UKM), Selangor, Malaysia
[e] Department of Civil and Environmental Engineering, South Dakota School of Mines & Technology, Rapid City, SD, United States

HIGHLIGHTS

- The composition of waste materials used to prepare AAB are reviewed.
- The properties of alkaline activator and its impact on AAB concrete are discussed.
- The fresh state properties of AAB concrete are reviewed.

ARTICLE INFO

Article history:
Received 6 March 2020
Received in revised form 29 May 2020
Accepted 1 June 2020
Available online 28 June 2020

Keywords:
Alkali-activated bindes
Precursors
Activators
Flow
Consistency
Slump
Setting time and heat of hydration

ABSTRACT

Alkali-activated binders (AAB) have been extensively researched as a potential replacement of ordinary portland cement (OPC) concrete to minimize carbon emissions released during OPC production while reusing a significant amount of industrial waste by-products. This paper provides a comprehensive review on the materials composition and the fresh properties of AAB. The chemical, physical, and mineralogical properties of a suite of pozzolans used to make AAB are analysed including fly ash, slag, metakaolin, silica fume, rice husk ash, palm oil fuel ash, and others. Sodium and potassium based alkaline activator solutions are also highlighted. The influence of AAB properties on workability (namely consistency, flow, and slump), setting time, reaction kinetics (as measured by isothermal calorimetry), and temperature are synthesized from past literature. The findings show that fresh properties of AAB can be tailored for specific applications based on mix design and processing conditions.

Contents

* Corresponding authors.
E-mail addresses: manjur.elahi@intertek.com (M.M.A. Elahi), md.maruf.hossain@uon.edu.au (M.M. Hossain).

https://doi.org/10.1016/j.conbuildmat.2020.119788
0950-0618/

1. Introduction

Rapid infrastructure development has increased the demand for cement production across the world. This increased cement production has been a major contributor to greenhouse gas emissions, which are released during its manufacture [1]. In fact, every tonne of cement production roughly produces 0.87 tonne of carbon dioxide, which accounts for approximately 6–7% of anthropogenic CO_2 emissions along with a significant reduction of natural resources [2–4]. As a result, the cement industry seeks to minimize both energy consumption and carbon footprint and is actively seeking for alternatives to ordinary portland cement (OPC). Furthermore, limited storage capacity and uncontrolled disposal of waste materials or industrial by-product into the landfill has become a growing concern to protect the environment [5]. Proper utilization of such by-products has countless benefits including increasing the conservation of natural resources, conservation of energy and environment, and resolving waste management issues.

To aid in this effort, there has been increased interest in the development of alkali-activated binders (AAB), which are made by mixing solid aluminosilicate powders, such as fly ash (FA), ground granulated blast furnace slag (GGBS), metakaolin (MK), rice husk ash (RHA), and palm oil fuel ash (POFA) with an alkaline solution [6–8]. The alkali-activated binder (AAB) is called with other terms such as "geopolymers" and "inorganic polymers" based on the physiochemical properties of the source materials and the type of alkali activator [9]. However, only alkali-activated binder (AAB) will be used throughout this review to avoid this ambiguity. Studies have estimated that the replacement of OPC by AAB can reduce the CO_2 footprint due to OPC manufacturing around 80% [9]. Concrete made with AAB have been shown to have excellent or equivalent physical properties to those made with OPC [8], including the compressive strength [10–12], setting time and hardening [13], reduced shrinkage [14], better thermal properties [15], freeze–thaw resistance [16], alkali-silica reactivity [17] and improved durability [18–21].

There are numerous industrial by-products, agricultural waste, and other less familiar waste products that have been used as a source of aluminosilicate materials. However, fly ash and GGBS are the most prevalent source materials, which have been broadly studied. Both of these AAB types can result in low permeability, high thermal resistance, acid resistance, and high compressive strength [13,22,23]. Apart from the types and properties of raw materials, the nature and molarity of alkali activator and curing temperature have a substantial effect on the overall properties of concrete made with AABs [24]. Studies conducted on AA slag [25] and AA metakaolin [25,26] have shown that higher mechanical strength can be achieved with increased concentration of the activators, and the strength of FA-based concrete depends on the optimum molarity of the activator used [27,28]. The nature of the alkaline solution can also influence the slag-based AAB mortars as investigated elsewhere [29]. For instance, sodium silicate as an activator enhances the polymerization process resulting in a silica-rich reaction product and improves the strength as stated in many studies [27,30]. In addition, Fernandez and Palomo reported more than twice as much strength for FA-based concrete when activated by NaOH and waterglass in combination instead of NaOH alone [31,32]. Furthermore, the solution modulus (molar ratio of SiO_2/Na_2O) [27,32], molar ratio of waterglass to sodium hydroxide [33], and liquid to binder (L/B) ratio [32] are some other crucial factors that dictate the properties of concrete made of AABs. On the other hand, the curing conditions has a significant impact mostly on the hardened properties of the AAB concrete as stated in literature [34–36].

1.1. Significance of the study

A significant body of research has shown that the properties of concrete made of AABs depends on many factors including the physical and chemical composition of source materials, the type and concentration of the alkaline solution, the mixing proportions and curing regimes. Most of the research has focused on the microstructure and mechanical properties of hardened concrete and durability aspects in different aggressive environments. There have been a number of review articles published on these aspects of AABs. To the best knowledge of these authors, there is not any comprehensive literature review which elaborately has discussed the fresh properties of AAB concrete. This undertaking has considered the fresh properties aspect of AAB concrete to fill the gap in the body of knowledge on this topic in addition to a review on material composition. Understanding the fresh properties such as workability (includes normal consistency, flow and slump) and setting time, heat of hydration and the surface temperature of freshly made concrete is a key factor for placeability in the field, early and later age strength and resistance against different durability issues. Therefore, a comprehensive review on the fresh properties of AAB concrete will add valuable information for future study in this area.

2. Constituents of alkali-activated binders

2.1. Raw materials

Portland cement is not required to produce alkali-activated binders. The two key ingredients of alkaline binders are: (1) alkaline solutions (for example, sodium hydroxide, sodium silicate, potassium hydroxide, and potassium silicate), and (2) aluminosilicate sources, which may have high calcium contents (for instance, industrial by-products such as fly ash, blast furnace slag, and agro waste such as rice husk ash, palm oil fuel ash). Similar to OPC concrete, fine and coarse aggregates are also required if using the AAB to make concrete.

2.1.1. Aluminosilicate precursors

The industrial by-products including fly ash, blast furnace slag, and silica fume and the agricultural by-products including rice husk ash, palm oil fuel ash and sugarcane bagasse ash, and calcined clay-based material known as metakaolin are some of the most common sources of aluminosilicate materials in the field of alkali-activated binders [37–39]. Other non-traditional source materials including coal and biomass ash [28], non-kaolinite-based clays [40–43], mine tailing from mining industry [44,45], red mud from aluminium extraction [46–50], diatomite [51], volcanic ash [52], co-fired ash [28], natural pozzolans [53] and other minerals [54–56] shown to have equivalent performance as alkaline binders compared to classical precursors. Industrial wastes such as magnesium-nickel slag, lead slag, copper-nickel slag are some other cementing supplements used in the fly ash-based system [46,57]. The commonality of these materials is that they consist of silica, alumina, iron, magnesium and calcium, which promotes the overall reaction mechanism in the alkaline binder system [57].

The most common solid aluminosilicate raw material is the fly ash, which is captured during the coal combustion process in electricity generation plants. The approximate annual production of fly ash is one billion tons, which can introduce environmental problems if not stored and disposed properly [58]. Class F fly ash is considered as an ideal source of aluminosilicates considering its abundance and price, spherical structure, and the significant presence of highly reactive phases. The majority of the fly ash used as an aluminosilicate sources material fall into Class F [59–62]. In contrast, high calcium fly ash as referred as Class C is not widely used as an alkaline binder's precursor due to faster setting [63,64] and availability [65]. Ground-granulated blast furnace slag, which is a by-product produced from pig iron manufacturing is another important source of aluminosilicate precursor for AAB systems. GGBS is frequently combined with Class F fly ash to improve the reactivity of these low calcium fly ash alkaline binders [66]. However it can be used alone as a precursor in alkaline binder systems, which have exhibited superior mechanical and microstructural properties as examined in some studies [67,68]. GGBS is high in calcium followed by silica and alumina which accelerate the reaction of alkaline binders [69].

Rice husk ash is a major agricultural by-product, which also has disposal challenges, consisting of high silica content, that has been researched as a precursor for AABs. It can have excellent pozzolanicity, which has been used for manufacturing special concrete [68,70]. RHA is burnt at a specified temperature range to produce the ash which is mainly comprised of amorphous silica [71,72]. The composition of this ash depends on the temperature and method followed in the incineration process [73]. RHA used in AABs found to influence the hydration heat of the mixture [74], enhances the workability and reduces the porosity [75], increases the compressive strength and decreases the permeability of concrete [68]. Palm oil fuel ash (POFA) is one of the major agricultural wastes produced through the combustion of palm oil husk and palm kernel shell after initial drying process is completed. The temparature and method for drying and incineration varies based on the raw palm oil husk as reported in some studies [76,77]. This agro waste produced in a large scale mostly in South East Asian countries, has shown a potential source of aluminosilicate in the production of AABs [78–80]. POFA is rich in silica and calcium that has recently been tested as an aluminosilicate source [79,80]. So far, it has been used as a part of binary and ternary mixes with other conventional pozzolans to produce alkali-activated binders [81–83].

Another common clay based anhydrous precursor used in producing alkaline binder is known as metakaolin [84–86]. Metakaolin is highly reactive supplementary cementitious material rich in alumina and silica produced by calcining high-grade kaolinite clay in the range from 600 °C to 800 °C with different drying cycle times [87]. During the calcination process, the chemically bound water in the kaolinite clay evaporates which breaks down the raw material's structure and eventually forms an amorphous phase known as metakaolin [88]. Kaolinite clay is abundantly available in different regions of the world [89], but in the construction industry it is used either as an alternative for clinker or an SCM [90]. The CO_2 emissions during the calcination of kaolinite clay to produce metakaolin is 5–6 times less than the temperature in OPC manufacturing, thus it is more environmentally friendly [91]. In addition, a higher mechanical strength was reported in metakaolin-based alkaline binders [86].

2.1.2. Alkaline solutions

Any substances that supplies alkali cations, which raises the pH level and facilitates the dissolution process can be considered as an alkaline solution [92]. The most commonly used activators are sodium hydroxide (NaOH), potassium hydroxide (KOH), sodium silicate (Na_2SiO_3) and potassium silicate (K_2SiO_3). Generally, NaOH and Na_2SiO_3, and KOH and K_2SiO_3 are used alone or in a combination based on the raw materials (precursor) and mix design requirements [93,94]. These solutions extract the silicon and aluminium atoms from the source materials to form polymeric silicon-oxygen-aluminium bonds as the polymerization process takes place [95,96]. Studies revealed that the NaOH has greater capacity liberating the silica and alumina monomers than KOH even though KOH is more alkaline in nature [97]. The polymerization process becomes faster in the presence of soluble silicates associated with Na or K than in the presence of alkaline hydroxide alone [93]. In NaOH and Na_2SiO_3 mixtures, a different molar concentration of NaOH is used and the final solution mod-

Table 1
Specific gravity of different pozzolans and OPC.

Pozzolans	Specific gravity	Reference
GGBS	2.89	[112]
	2.68	[113]
	2.80	[114]
	2.85	[82]
RHA(G)	2.30	[112]
	2.23	[113]
	2.28	[115]
	2.15	[116]
	2.08	[82]
RHA(UG)	1.94	[82]
POFA(G)	1.89	[117]
	2.22	[118]
	2.31	[82]
POFA(UG)	2.16	[82]
FA	2.20	[119]
	2.05	[120]
	2.33	[121]
	2.18	[117]
	2.34	[114]
MK	2.50	[112]
	2.40	[122]
SF	2.22	[123]
NPOFA	2.52	[124]
WTS	2.61	[116]
FP	2.55	[125]
CP	2.53	[125]
WCP	2.61	[126]
OPC	3.14	[82]

Pozzolans: GGBS: Ground granulated blast furnace slag; POFA: Palm oil fuel ash; FA: Fly ash; MK: Metakaolin; SF: Silica fume; NPOFA: Nano POFA; WTS: Water treatment sludge; FP: Fluorescent lamp glass; CP: Container glass; WCP: Waste ceramic glass; OPC: Ordinary portland cement.

ulus as defined by the molar ratio of SiO_2/Na_2O [98]. This solution modulus of commercially available solid Na_2SiO_3 ranges between 0.93 and 3.32 as reported in many studies [60,99,100]. Similarly, potassium hydroxide and/or potassium silicate was also utilized as an activator in studies performed by Al Majidi [101] and Zhang [102]. Karim et al. used 2.5 M KOH, NaOH and $Ca(OH)_2$ in developing a zero-cement binder from different aluminosilicate sources where NaOH offered better performance compared to other activators [103].

In addition to the most commonly used alkaline activators, there are different materials/solutions that have been extensively investigated to evaluate the potential to use as alkaline activator. The appropriateness of Na_2CO_3 as an alkaline solution for GGBS-based binder has been studied in some studies [104,105]. Bernal and Provis studied the effectiveness of sodium carbonate over sodium silicate as an alkaline solution in a slag-based AAB system [106]. These authors observed a higher setting time and improved workability with sodium carbonate than sodium silicate. Moreover, red mud was used as a source of sodium hydroxide [107]. Li et al. [108] used alkaline earth cation based sources such as calcium oxide, magnesium oxide, dolomite, and calcium hydroxide as alkali suppliers, which have facilitated the reaction process. In another study, Kim et al. observed CaO powder as more efficient activator for slag-based binders than $Ca(OH)_2$ [109].

2.2. Composition of pozzolans

Different physical and chemical properties of the pozzolans including the specific gravity, particle size distribution, fineness, oxide compositions, crystallographic structure, and morphology are examined here.

2.2.1. Physical properties of pozzolans

Specific gravity of different pozzolans, as found in literatures, is presented in Table 1. The table shows that all these pozzolans are less dense than the OPC. The specific gravity of pozzolans in a variety of literature lies between 1.89 and 2.89, as compared to cement at 3.154. Processing, such as, grinding has a considerable effect on the specific gravity of pozzolans as examined by Karim et al. [82]. For example, ground rice husk ash (RHA-G) and palm oil fuel ash (POFA-G) have comparatively higher specific gravity compared to unground (UG) as shown in Table 1. This effect was also discussed in other studies [110,111].

The fineness and particle size distribution of raw aluminosilicate materials have a substantial influence on hydration, strength development, and durability of AAB concrete. Fineness as presented in terms of median grain size (D_{50}), blaine fineness (m^2/g) and percent passing through mesh size 45 μm (#325 sieve) in literatures is presented in Table 2. Finer particles increase the rate

Table 2
Particle size and fineness of different pozzolans and OPC.

Materials	Grain size (μm) d_{50}	Fineness (m^2/g) Blaine	Passing through 45 μm sieve (%)	Reference
Slag	–	3.27	–	[111]
	10.8	–	89	[127]
	15	–	–	[128]
	–	0.405	–	[112]
	–	0.400	–	[114]
FA	–	–	89	[129]
	9.67	–	–	[130]
	–	0.463	–	[131]
	–	–	93	[120]
	1.46	–	–	[132]
	16.23	2.96	–	[133]
	45	–	–	[134]
	3.43	–	83.25	[121]
	16.23	2.96	–	[115]
	–	0.600	–	[114]
POFA (G)	16.7	–	–	[130]
	22.78	12.92	–	[133]
	–	0.915	–	[111]
	45	–	–	[134]
	22.78	12.92	–	[117]
	–	0.520	–	[118]
	16.08	0.458	–	[82]
POFA (UG)	57.13	0.197	–	[82]
RHA(G)	–	2.98	–	[112]
	7.0	–	–	[113]
	16.76	67.33	–	[115]
	6.63	0.695	–	[82]
RHA(UG)	8.65	0.575	–	[82]
MK	3.50	–	–	[127]
	0.011	–	–	[132]
	12.66	–	–	[135]
	–	4.31	–	[112]
	2.55	–	–	[122]
BA	39.60	–	90	[136]
	50.00	–	–	[137]
SF	0.004–0.016	–	–	[120]
	0.650	–	–	[123]
NPOFA	0.982	1.96	–	[124]
FP	4.65	10.03	97.84	[125]
CP	11.72	5.89	96.55	[125]
WCP	35	12.2	–	[126]
OPC	16	0.203	–	[82]

Pozzolans: GGBS: Ground granulated blast furnace slag; POFA: Palm oil fuel ash; FA: Fly ash; MK: Metakaolin; SF: Silica fume; NPOFA: Nano POFA; BA: Bottom ash; WTS: Water treatment sludge; FP: Fluorescent lamp glass; CP: Container glass; WCP: Waste ceramic glass; OPC: Ordinary portland cement.

Table 3
Oxide composition of pozzolans and OPC.

Materials	Oxide compositions (wt. %)												Reference
	SiO_2	Al_2O_3	Fe_2O_3	CaO	MgO	SO_3	Na_2O	K_2O	P_2O_5	TiO_2	MnO	LOI	
FA (Class F)	50.70	28.80	8.80	2.38	1.39	0.30	0.84	2.40	–	–	–	3.79	[142]
	61.89	28.05	4.11	0.87	0.38	1.32	0.40	0.82	–	–	–	0.49	[119]
	53.50	28.80	4.47	1.55	0.81	0.14	0.77	–	–	–	–	3.11	[143]
	55.90	21.80	6.62	4.91	2.00	0.32	0.32	2.20	–	–	–	–	[130]
	55.23	21.43	7.42	7.94	2.61	0.81	–	–	–	–	–	1.66	[144]
	48.80	27.00	10.2	6.2	1.4	0.22	0.37	0.85	1.2	1.3	0.15	1.7	[129]
	64.97	26.64	5.69	0.33	0.85	0.33	0.49	0.25	–	–	–	0.45	[120]
	27.35	50.85	2.01	5.41	0.28	–	0.04	0.33	–	2.12	0.02	7.74	[132]
	54.72	27.28	5.14	5.31	1.10	1.00	0.43	1.00	1.11	1.81	0.09	6.8	[133]
	57.60	28.90	5.80	0.20	0.90	0.20	–	0.90	–	–	–	3.6	[134]
FA (Class C)	23.50	13.80	4.80	23.20	4.20	5.90	6.30	0.40	–	–	–	0.15	[140]
	20.60	14.50	4.70	29.90	6.20	3.80	2.50	0.30	–	–	–	0.32	[140]
	29.50	17.30	6.50	30.60	5.30	3.50	3.10	0.40	1.30	1.60	–	0.23	[139]
Slag	34.10	13.50	0.36	11.83	4.19	–	–	–	–	–	0.20	1.4	[111]
	35.23	12.33	0.85	40.10	8.00	–	0.25	0.50	–	–	–	1.40	[54]
	34.95	12.63	–	45.10	–	–	0.22	1.24	–	–	–	–	[127]
	37.50	7.27	0.73	38.48	10.86	0.39	0.64	0.26	–	–	–	2.13	[144]
	52.75	18.05	5.92	12.92	3.86	1.76	1.11	2.09	–	1.01	0.14	1.60	[128]
	35.80	13.21	1.97	35.68	9.76	0.21	0.48	0.57	–	–	–	2.32	[113]
	33.05	16.36	0.53	45.0	6.41	1.21	0.13	0.42	–	–	–	3.05	[82]
RHA	89.47	0.83	0.53	0.68	0.37	0.12	0.22	0.17	–	–	–	7.61	[113]
	89.34	0.45	0.40	0.76	0.49	0.90	–	4.98	2.58	–	0.02	–	[115]
	93.46	0.58	0.52	1.03	0.515	0.60	0.08	1.82	1.60	–	–	7.76	[112]
	89.17	–	0.41	0.61	1.22	–	1.22	1.12	–	0.03	–	0.15	[116]
	87.75	0.38	0.19	1.04	0.69	0.56	0.05	2.83	1.31	0.02	0.07	3.04	[82]
POFA	47.37	3.53	6.19	11.83	4.19	–	–	–	–	0.24	–	1.84	[111]
	44.40	1.20	2.10	10.30	9.13	5.80	0.55	12.40	–	–	–	–	[130]
	64.17	3.73	6.33	5.80	4.87	0.72	0.18	8.25	5.18	0.19	0.18	6.30	[133]
	63.40	5.5	4.20	4.30	3.70	0.9	–	6.30	–	–	–	6.00	[134]
	47.22	2.24	2.65	6.48	5.86	9.19	1.22	11.86	5.37	0.17	0.10	5.42	[82]
SF	93.67	0.83	1.30	0.31	0.84	0.16	0.40	1.10	–	–	0.84	2.10	[142]
	94.90	049	1.7	0.56	0.70	–	–	–	–	–	–	1.61	[54]
	94.49	0.07	0.10	0.50	0.62	0.11	0.09	0.54	–	–	–	3.21	[145]
	93.67	0.83	1.30	0.31	0.84	0.16	0.40	1.10	–	–	0.84	2.10	[123]
MK	54.77	29.65	1.57	0.18	0.51	–	0.19	0.64	–	–	–	1.23	[54]
	55.54	44.16	–	0.08	–	–	0.05	0.90	–	–	–	–	[127]
	53.32	21.72	2.25	0.09	0.21	–	0.49	0.64	–	0.63	0.02	0.08	[135]
	51.70	40.60	0.64	0.71	0.96	0.10	0.31	2.00	3.00	0.20	0.08	1.19	[112]
	52.14	41.88	1.35	0.42	0.38	–	–	1.10	–	1.30	–	1.10	[146]
	51.30	44.42	0.42	0.05	0.01	0.13	0.33	0.14	–	1.69	–	1.30	[122]
BA	57.00	24.00	8.00	1.71	1.10	–	2.90	–	–	0.80	1.72	3.30	[136]
	54.00	25.00	4.00	5.00	2.00	3.00	–	1.00	1.00	2.00	–	2.00	[137]
NPOFA	67.3	4.12	8.12	3.97	2.72	0.53	0.11	8.45	2.47	0.22	0.07	–	[124]
WTS	58.99	24.64	6.63	0.69	1.14	–	4.08	1.54	–	0.88	–	–	[116]
FP	68.80	2.40	0.11	7.43	2.70	0.19	15.18	1.42	0.64	–	–	0.66	[125]
CP	70.30	1.90	0.42	12.30	1.68	0.07	12.80	0.23	–	–	–	0.68	[125]
WCP	72.60	12.2	0.56	0.02	0.99	–	13.46	0.03	–	–	–	0.13	[126]
OPC	20.99	4.60	4.44	67.17	2.53	2.98	0.03	0.16	–	–	–	1.30	[82]

Pozzolans: GGBS: Ground granulated blast furnace slag; POFA: Palm oil fuel ash; FA: Fly ash; MK: Metakaolin; SF: Silica fume; NPOFA: Nano POFA; WTS: Water treatment sludge; FP: Fluorescent lamp glass; CP: Container glass; WCP: Waste ceramic glass; OPC: Ordinary portland cement.

of hydration by providing better particle packing and by increasing nucleation sites, which ultimately leads to increase in strength. For these reasons, pozzolans are ground to obtain higher fineness for use. Similar to that observed for specific gravity, a significantly higher fineness in POFA (more than double in surface area) and RHA was observed after grinding the raw pozzolans [82,111]. The fineness or median particle size (D_{50}) for each of the pozzolans reviewed from literatures varies significantly as tabulated in Table 2. It can be noted that the blaine fineness (m^2/g) of all of those reported (except POFA-UG) was higher than the OPC.

2.2.2. Oxide composition of pozzolans

The oxide composition of different pozzolans investigated using X-ray fluorescence (XRF) is presented in Table 3. The oxide composition and ignition loss test results of thirteen different commonly used pozzolans are categorized here. The pozzolans possess a high amount of silica and alumina as expected for precursor materials. As seen from Table 3, the chemical constituents of FA studied here mostly consists of silicon dioxide and aluminium oxide and all of them meet the minimum 50% major oxide (SiO_2, Al_2O_3, and Fe_2O_3) requirement to fall into Class F pozzolans according to ASTM C618 [138] with few exceptions which are classified as Class C fly ash due to high calcium contents [139,140]. On the other hand, the agricultural by-products such as rice husk ash and palm oil fuel ash are predominantly composed of silicon dioxide. Although the oxide composition of RHA meets the major oxide requirement of 70% (minimum) as per ASTM C618 to fit under Class N pozzolan POFA does not meet this requirement [138]. POFA contains a high proportion of K_2O compared to other pozzolans which can be attributed to the higher consumption of K_2O of palm oil tress throughout the cultivation period [82]. The high amount of CaO in POFA is the result of the availability of calcium oxide in lime and fertilizers [141]. Similarly, silica fume is mainly composed of silicon dioxide, metakaolin and bottom ash are mainly composed of silicon and aluminium dioxide and some other uncommon waste materials are mostly consist of SiO_2 and Al_2O_3 as tabulated in Table 3.

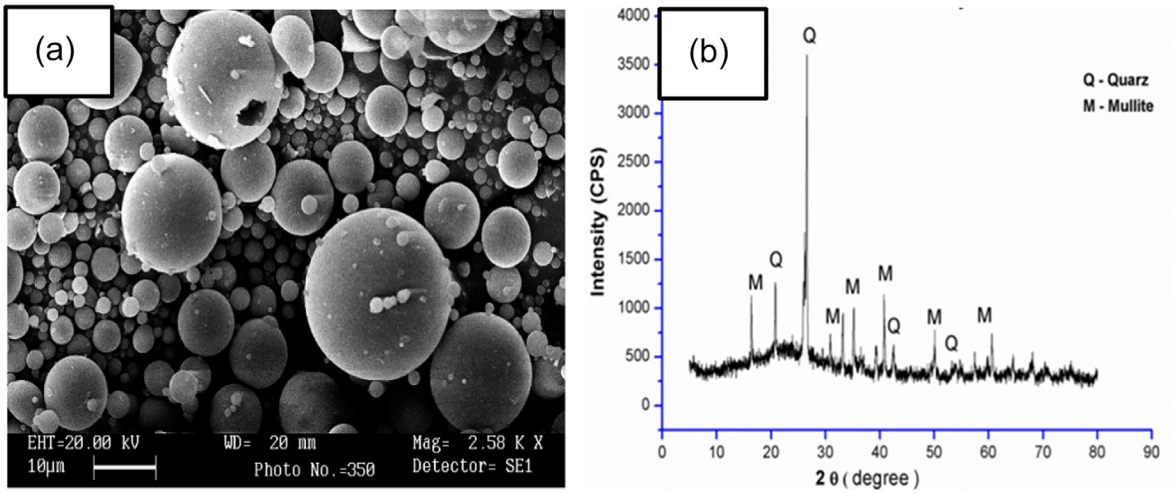

Fig. 1. SEM (a) [150] and XRD (b) [151] of fly ash (adapted).

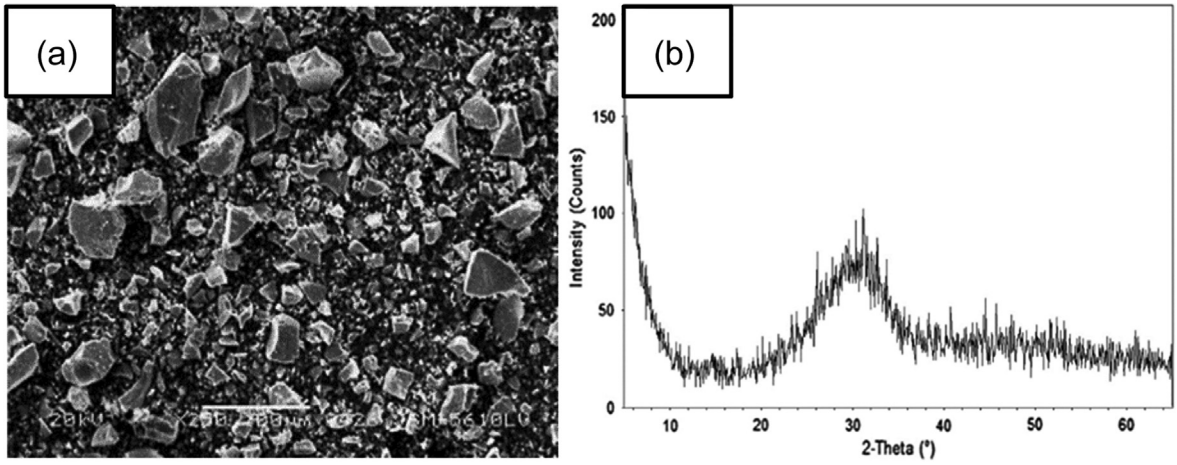

Fig. 2. SEM (a) [153] and XRD (b) [154] of GGBS (adapted).

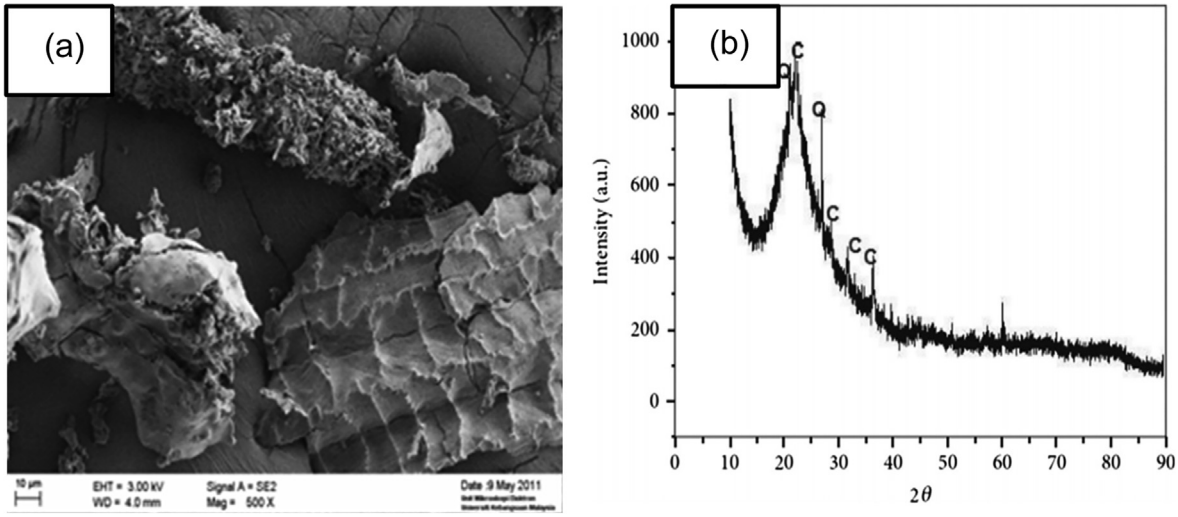

Fig. 3. SEM (a) [82] and XRD (b) [155] of RHA (adapted).

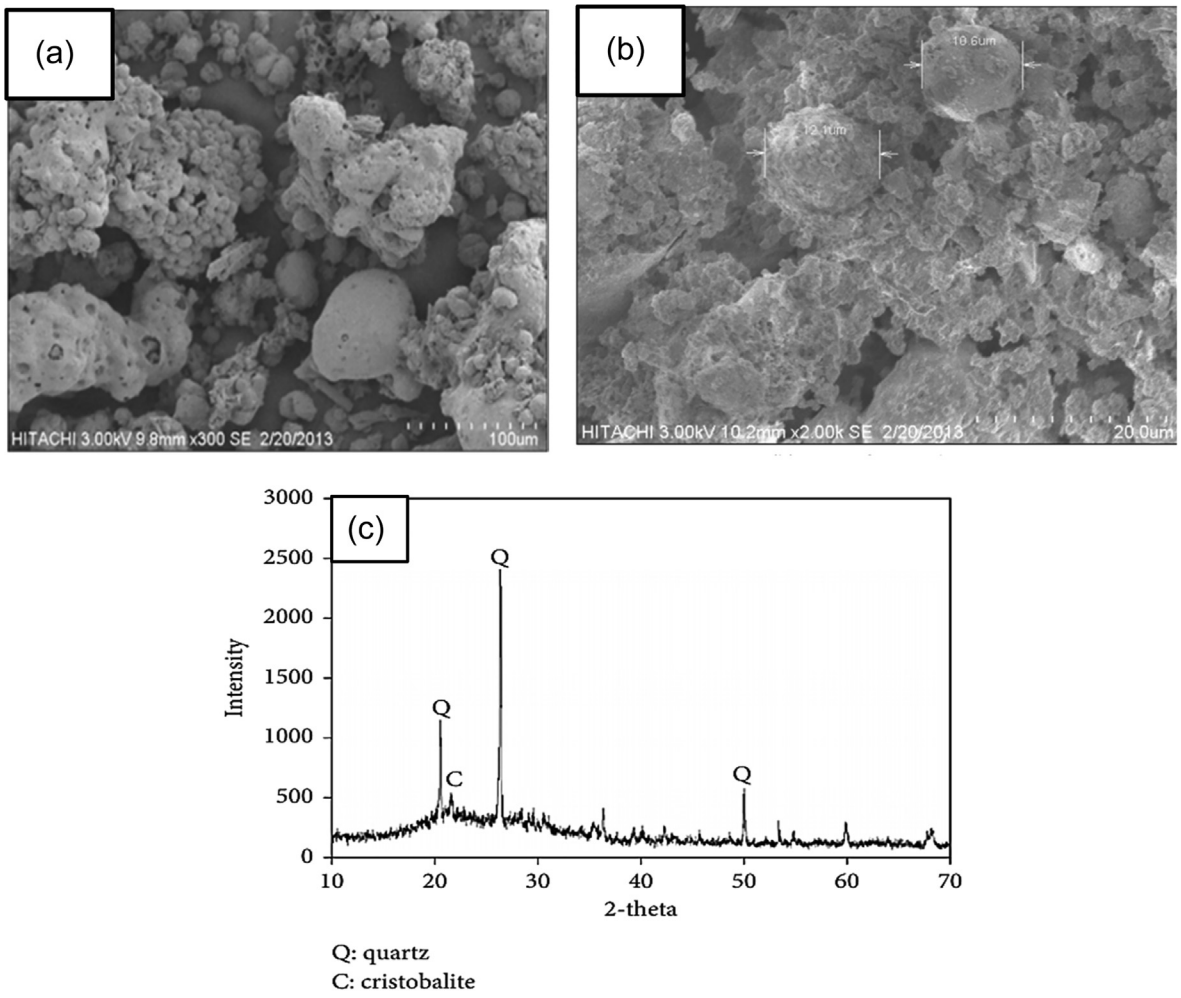

Fig. 4. SEM of unground (a) and ground (b) and XRD of POFA (c) [111] (adapted).

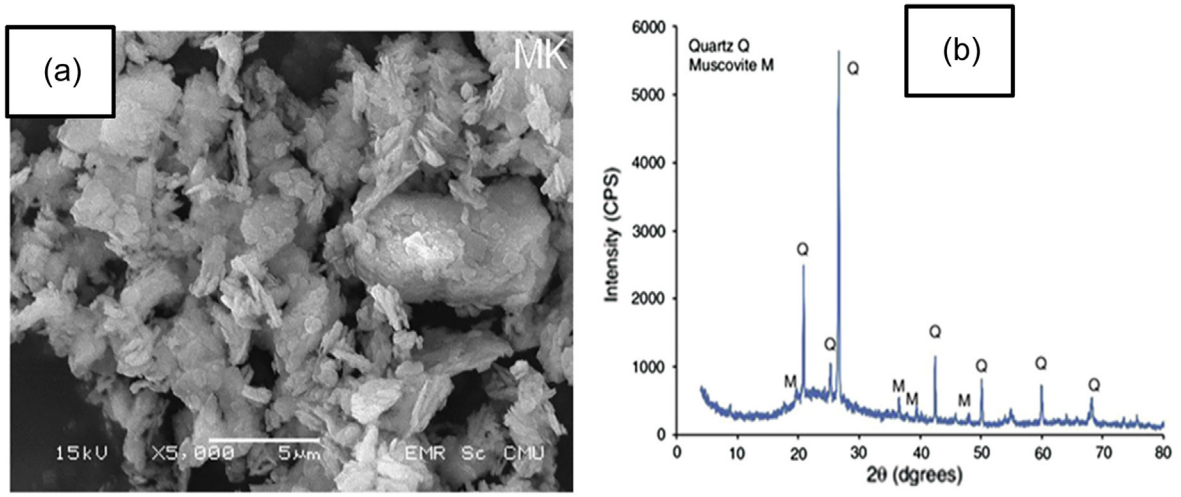

Fig. 5. SEM (a) [122] and XRD (b) [165] of metakaolin (adapted).

2.2.3. Morphology and mineralogy of pozzolans

The size and shape of the pozzolans is one of the most important factors for activation with the alkaline solution, bonding, flow and workability of AABs. Generally, particle shape is examined through Scanning Electron Microscopy (SEM) analysis. In addition to this, the crystalline phases and amorphous content of the materials are analysed using the X-ray diffraction (XRD) technique. The morphology and mineralogical analysis of the pozzolans reported in literature are discussed below.

2.2.3.1. Fly ash. FA can react with all types of alkaline solutions to produce aluminosilicate binders [147]. Fig. 1-a depicts the SEM

pictogram of FA which are mainly spherical in shape, enhancing better flow in the mixtures and improving the workability. The XRD peaks show crystalline phases in fly ash as indicated by sharp peaks of quartz and mullite (alumina silicate) in addition to an amorphous hump as illustrated in Fig. 1b. Similar micrographs and crystallography of fly ash was observed in other studies [148,149].

2.2.3.2. Ground-granulated blast furnace slag (GGBS). The SEM picture of slag demonstrates an irregular, angular, along with spherical particles with a smooth surface as shown in Fig. 2a. It was also found to have square and diamond shaped particles in other studies [82,152]. The XRD pattern of slag indicates an amorphous phase mostly consisting of glassy materials as shown in Fig. 2b. Some studies also reported this as amorphous phase with minor magnetite [152] and amorphous phase with silica [82,111].

2.2.3.3. Rice husk ash. The SEM picture shows that RHA consist of a porous and spongy structure, which is mainly angular and cellular in shape as presented in Fig. 3a. The XRD pattern of RHA is mainly dominated by quartz at 2θ = 20.75° and 26.8° and cristobalite at 21.7°, 28.9°, 31.2° and 36° as shown in Fig. 3b. Karim et al. also reported cristobalite and sylvite as the major crystalline phases [82]. These crystalline phases were also reported in other studies [156,157].

2.2.3.4. Palm oil fuel ash. Fig. 4a and b show the SEM micrograph of unground POFA and POFA after grinding, respectively. The unground POFA is mainly composed of irregular particles with honeycomb like porus surfaces which change to a more spherical shape after grinding as shown by Salih et al. [80]. The changes in the surface texture is also observed in some other studies [82,158–160].

The crystallinity as detected by XRD of POFA shows that its mostly composed of amorphous silica with some sharp peaks ranges from 20° to 40°(2 theta) as depicted in Fig. 4c [161]. Karim et al. reported this crystalline phase as quartz and mullite [82]. However, other studies on micro POFA (rich in silica) reported quartz and cristobalite as the main crystalline phases [162-164].

2.2.3.5. Metakaolin. The SEM micrograph in Fig. 5a shows that metakaolin has a plate-like structure. The XRD pattern in Fig. 5b shows an amorphous phase hump, which is highly reactive when blended with alkaline solutions [166] and crystalline phases of quartz and muscovite.

2.2.3.6. Other non-conventional pozzolans. Bottom ash (BA) produced from coal-based power plants was shown to have irregularly shaped particles with some pore cavities as well as crystalline phases of quartz and mullite [136,137]. Water treatment sludge (WTS), which is a by-product of a water treatment plant was shown to be crystalline under XRD (rich in silica and alumina) with irregular particle shape [116] and offered a considerable strength when activated by sodium hydroxide and sodium silicate solution [116]. Tho-In et al. studied the strength and microstructure of AABs comprised of fluorescent lamp glass (FP) and ground container glass (CP) blended with fly ash and observed crystalline phases of silica and geometrically angular shaped particles [125]. Waste ceramic powder (WCP) has irregular and angular shaped particles with crystalline phases composed of quartz and mullite [126].

3. Fresh properties of alkali-activated binder

3.1. Normal consistency and flow

Understanding the rheology and workability, namely the consistency and flow behaviour of alkali-activated paste, mortars and concrete is crucial to enable successful casting or placement [85]. In this section, the consistency and flow behaviour of AAB's made with different pozzolans will be highlighted. Karim et al. studied the consistency and flow of paste samples of ternary blended binders activated by 5% NaOH (L/B = 0.50) containing ground and unground RHA and POFA and GGBS (ground) [82]. The results revealed that the paste specimens prepared with unground RHA and POFA demonstrate a higher consistency (water demand) than its corresponding ground and OPC samples as presented in Fig. 6 [82]. They concluded that the porous and spongy nature and the shape of the RHA and POFA particles was attributed for this change. It also shows that the consistency of paste increases with the increased RHA content. Higher consistency with increased RHA dosage was also found in another study [167]. Fig. 6 shows that the flow of OPC mortar is higher than all tested alkali binders even though superplasticizer was added to the AAB to increase the flow potentially due to its fineness, particle size and

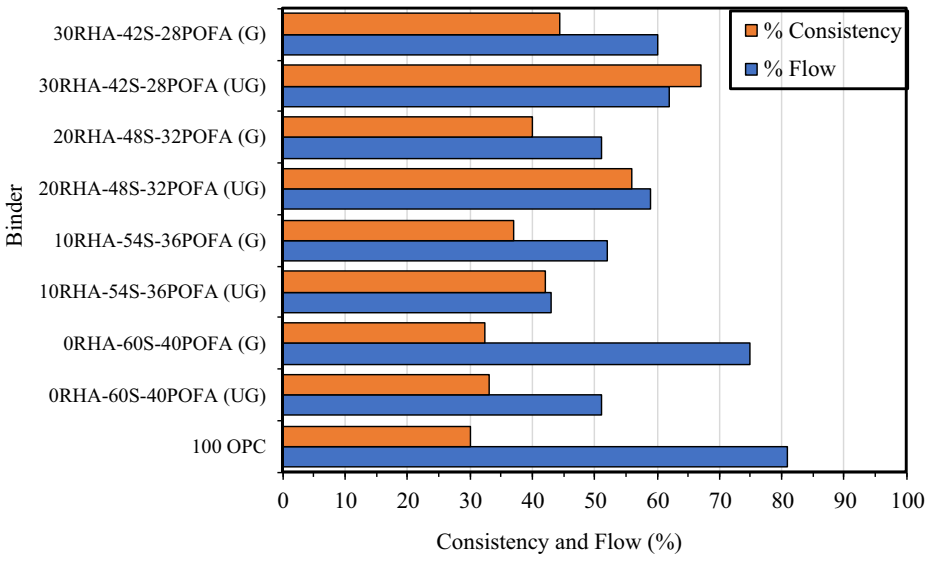

Fig. 6. Normal consistency (paste) and flow (mortar) of ternary blended AABs [82] (reproduced).

Table 4
Consistency of paste and flow of mortar of AA ternary blends with different activators [103] (reproduced).

Binder	Normal Consistency (%)	Flow (%) in different activators		
		$Ca(OH)_2$	KOH	NaOH
60S-40FA-0RHA	32.5	79	78	73
55S-35FA-10RHA	35.8	68	59	51
50S-30FA-20RHA	39.0	62	58	48
40S-30FA-30RHA	42.5	74	70	58
70S-20FA-10RHA	33.5	80	76	71
OPC	30.5	81		

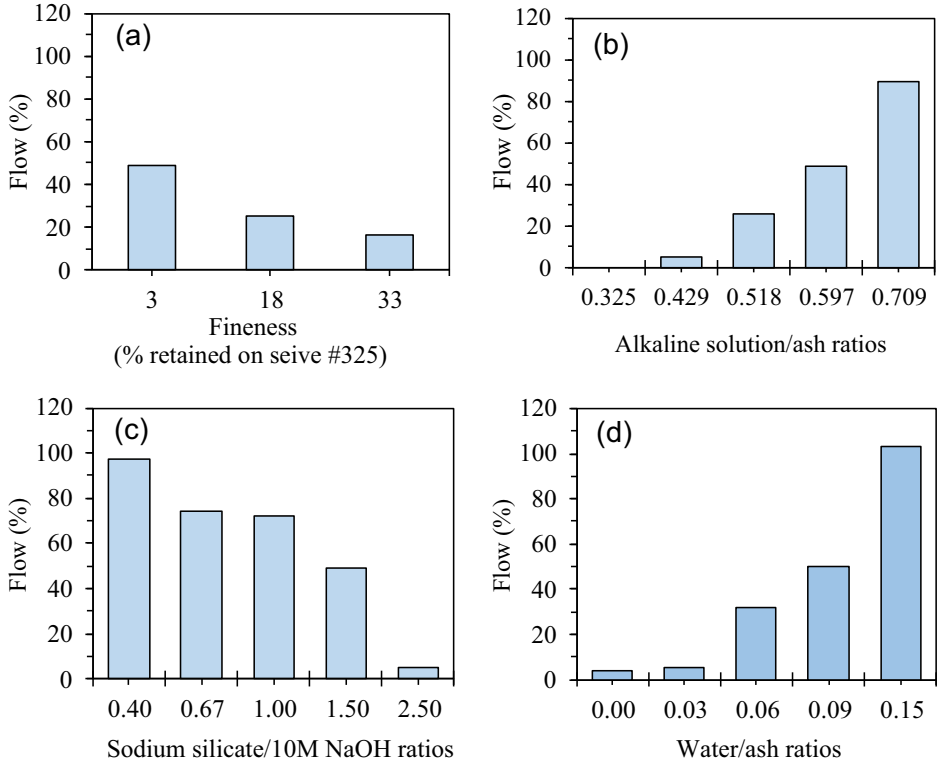

Fig. 7. Flow of alkali-activated bottom ash mortar with different fineness (a), solution to ash ratio (b), sodium silicate to sodium hydroxide ratio (c) and water to ash ratio (d) [181] (reproduced).

morphology and oxide composition of these pozzolans [82]. Compared to other pozzolans, the higher loss in ignition (LOI), larger surface area, and amorphous silica in RHA were referenced as the potential reasons for its lower flowability [112].

The consistency and flow of zero cement GGBS-FA-RHA blended pastes and mortars with different activator types was also compared with OPC [103]. The results presented in Table 4 shows that the consistency of all tested activated binders was higher than the OPC. Similar results were reported elsewhere [167]. In that study, the measured flow of the AABS mortars was less than the control OPC and the lowest flows were observed in binders activated with NaOH as shown in Table 4 [103]. This test results aligns with other studies, which found potassium-based activator provided better flowability than sodium-based activator [168,169]. Generally, when higher amounts of water is required to obtain the desired consistency, a decrease in flowability is observed [141,170].

Recently, Alanazi et al. examined the impact of slag, silica fume, and metakaolin addition to the flow characteristics of alkali-activated fly ash (AAFA) mortars with Na_2SiO_3 (SS) and NaOH (SH) with a molar ratio of SS/SH = 1 and 2.5 [145]. The experimental results revealed that the maximum measured flow was found for AAFA alone, which was referred to the spherical shape and slower reaction kinetics of FA [171]. However, the flow reduced with increased addition of the other pozzolans. For slag, the reduction of flow is attributed to their rough texture and faster reaction rate due to their higher calcium content [172,173]. In addition, high dosages of slag addition have resulted in significant flow reduction as stated in other studies [174,175].

Some other factors that dictate the flowability include the powder to alkaline solution ratio [176], the higher viscosity of sodium silicate compared to sodium hydroxide [177], the powder to sand ratio [178], the effect of Ca/Si ratio [179], and the molarity of the activator solution (e.g., NaOH) [180]. Sathonsaowphak et al. conducted a comprehensive study on the flow characteristics of lignite bottom ash-based activated mortars to determine the impact of ash fineness, solution to ash ratio, sodium silicate to hydroxide ratio and water to ash ratio as presented in Fig. 7(a–d) [181].

3.2. Slump

The workability of alkali-activated fresh concrete is a very important property, which can affect placement, but also later age properties. One measure of workability of fresh concrete is the slump test [171,182] and for the paste and mortar it is usually

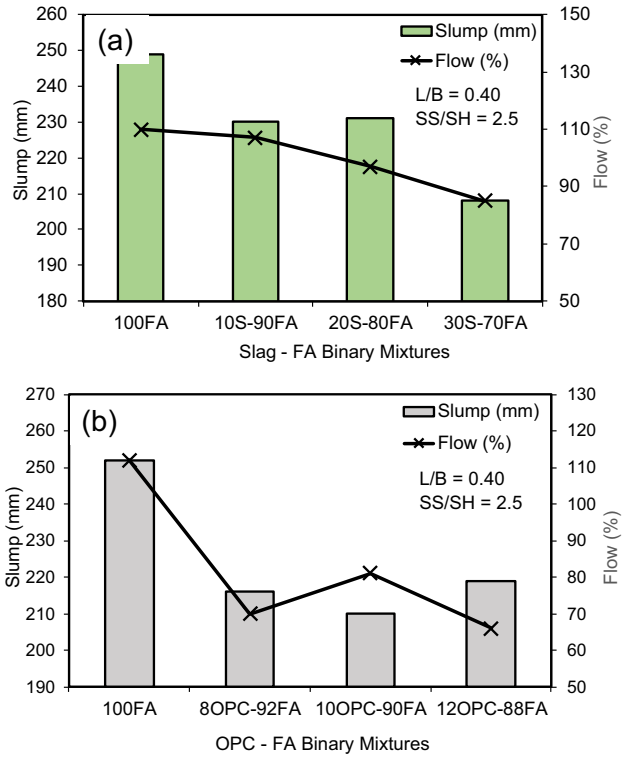

Fig. 8. Effect of GGBS (a) [171] and OPC (b) [182] addition on the slump of concrete and flow of mortar in fly ash-based activated binders (reproduced).

measured following the flow table procedure [152,183,184] or mini-slump test method [185]. When powders rich in calcium, such as GGBS or OPC, are added to fly-ash based AABs, a reduction in workability has been observed [101,179,186]. Nath and Sarkar studied the effect of slag and OPC inclusion into FA-based alkali-activated concrete and mortars and found a substantial reduction in slump and flow when GGBS and OPC was used to partially replace fly ash as presented in Fig. 8(a and b).

Similarly, Xie et al. studied the effect of water-binder ratio of FA-GGBS alkaline binders on workability and found reduced slump values due to GGBS replacement of fly ash [114]. The decreased workability can be explained due to the angular shaped GGBS particles compared to the spherical shaped FA particles and the accelerated hydration kinetics of the high calcium available in GGBS [187,188]. High calcium FA binders showed lower slump than OPC binders, which was attributed to the rapid hydration product growth [139].

The activator type has a pronounced effect on the workability of alkaline binders. For example, sodium silicate and sodium hydroxide influence the overall workability. The slump and flow decrease with increased Na_2SiO_3/NaOH (SS/SH), and superplasticizers and/or additional water must be used to improve workability as this ratio increases [189] as shown in Table 5. Similarly, the effect of SS/SH on the workability of FA-based binders replaced with 10% GGBS and OPC is shown in Fig. 9 [171,182]. The results show that the slump and flow both decreased with increased SS/SH. OPC replaced FA binders show a considerably greater reduction in slump and flow reduction. It can be concluded that SS/SH has a profound effect on the workability because of the high viscous nature of sodium silicate [185].

Similar to concrete and mortars, the workability of FA-based alkaline paste was found to reduce with the increased percentage of GGBS addition [174]. Fig. 10 shows the reduction in spread diameter (Fig. 10-b) of FA paste (Fig. 10-a). Similar results were found in another study [175,185].

3.3. Setting time

The setting time of alkali-activated binder is a critical factor that influences its ease of placement in the field. This workable time window is a crucial factor because it dictates the available time starting from batching, hauling to the jobsite, and final placement of concrete. The setting time test can be performed using the Vicat apparatus.

Setting behaviour is controlled by many factors including the, composition of the raw pozzolans, specimen preparation, use of additives, and curing regimes [191]. However, in alkali-activated concrete production, the proportion of alkaline activator to FA and ratio of sodium silicate to sodium hydroxide have been found to not have any profound impact on setting time [176]. On the other hand, longer setting times were observed using NaOH activator compared to Na_2SiO_3 activator in another experiment [192].

The initial and final setting time was found to decrease considerably with increased molarity of NaOH activator as shown in Fig. 11 [190]. Similar results were reported in another study [193].

The setting time of slag-based alkali binders was found to decrease with increasing calcium content as described using a conceptual SiO_2-Al_2O_3-CaO system, where Ca was considered as a network modifier accelerating the rapid dissolution of available precursors presented in Fig. 12 [194]. Li et al. reported a prolonged setting period when a high amount of fly ash and/or metakaolin was incorporated in the GGBS-FA and GGBS-metakaolin alkaline binders [195,196]. In addition, the slag addition has been shown to substantially reduce setting time in several studies [101,171,197–199]. Fig. 13 shows the decreases in setting time for different percentages of slag replaced alkaline FA-based pastes (Fig. 13a) [171]. Similar findings were reported in another study as shown in Fig. 13b [174].

Table 5
Additional water, superplasticizers and flow of fly ash-based geopolymer mortar [189] (reproduced).

Na_2SiO_3/NaOH	NaOH molarity	Flow (%)	Water (% of fly ash)	Superplasticizer (% of fly ash)
0.67	10	135 ± 5	0	0
1.0	10	125 ± 5	0	0
1.5	10	110 ± 5	0	0
3.0	10	110 ± 5	2.3	3
0.67	15	135 ± 5	3.4	3
1.0	15	125 ± 5	3.4	4
1.5	15	110 ± 5	3.4	5
3.0	15	110 ± 5	4.5	6
0.67	20	135 ± 5	6.8	12
1.0	20	125 ± 5	6.8	8
1.5	20	110 ± 5	6.8	10
3.0	20	110 ± 5	7.9	10

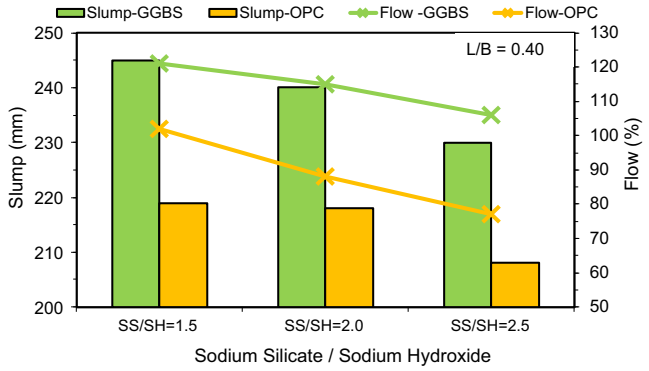

Fig. 9. Effect of sodium silicate to sodium hydroxide ratio on the slump and flow of GGBS-FA [171] and OPC-FA [182] based activated binders (reproduced).

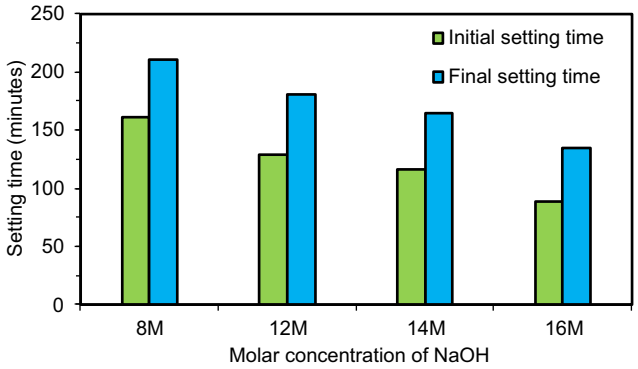

Fig. 11. Impact of NaOH molar concentration on the setting time of AAB [190] (reproduced).

Furthermore, the inclusion of calcium rich pozzolans such as GGBS and OPC into the metakaolin-based binders can have a profound effect on setting time as reported elsewhere [69,122]. Wianglor et al. examined a gradually decreasing trend in initial and final setting time when 5–30% of metakaolin binder was replaced by the equivalent OPC as shown in Fig. 14 [122]. This can be attributed to either the abundantly available SiO_2 and Al_2O_3 in metakaolin or an increase in CaO from the OPC. A similar observation was reported in another study [69]. However, compared to 100% MK, the inclusion of OPC increases setting time substantially. This can be explained due to the high fineness and plate-like morphology of metakaolin, which shows a faster polymerization as confirmed in other studies [200,201].

Karim et al. have extensively investigated ground and unground POFA/RHA based binders with different slag contents and observed a significant impact on setting time with added slag [82]. Some other studies on POFA-based binders which incorporated different dosages of slag confirmed a similar impact on the setting time [111,202]. As presented in Fig. 15, it can be seen that the setting time POFA-based binders with GGBS replacement has been remarkably decreased with increased slag content, which shows that the time required to set reduced to 77% when 50% slag added to the mixture compared to the 100% POFA.

While the slag has been found to control setting time, the inclusion of 5% ultrafine FA was also found to shorten the setting time significantly because of its very high specific surface area as reported by Deb and Sarkar [186]. The setting time of FA-based alkaline binder was also affected by the inclusion of nano silica particles activated by 12 M NaOH solution, which exhibited increased set time with increased dosage of nano silica as shown in Fig. 16 [203]. The effect of nano silica addition on setting behaviour of AABs was also reported by Zhan et al. [204].

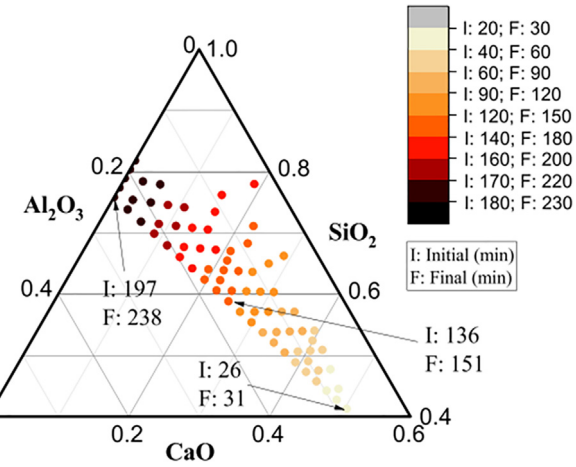

Fig. 12. Setting time of alkali-activated materials based on SiO_2-Al_2O_3-CaO system [194] (adapted).

3.4. Reaction kinetics

Differential Scanning Calorimetry (DSC), which measures the difference in heat required to increase the temperature and Isothermal Calorimetry (IC), which measures the heat flow at a fixed temperature, are the most widely used methods to study

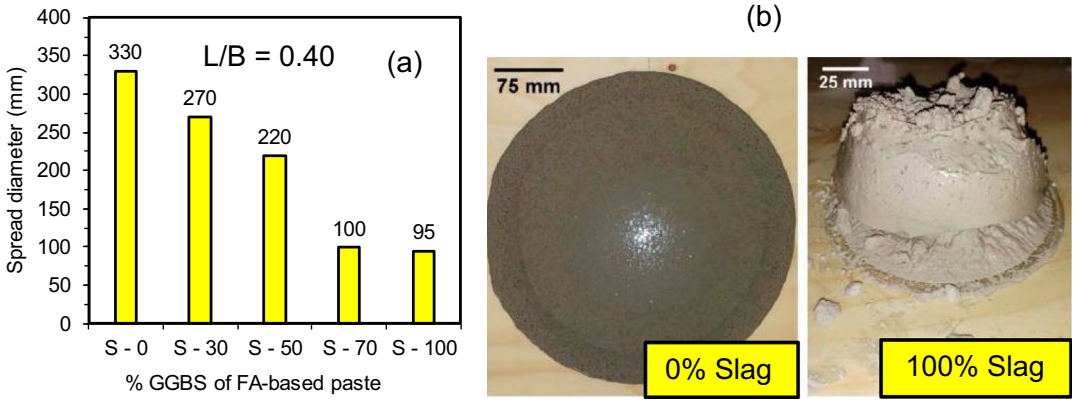

Fig. 10. Mini slump spread diameter of different percent of slag replaced FA-based paste (a) and mini slump test pictures (b) [174] (reproduced and adapted).

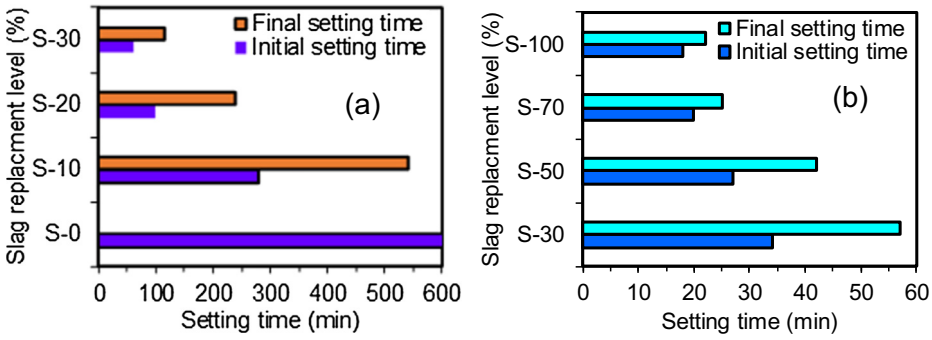

Fig. 13. Influence of GGBS on setting time of FA-based binders [171,174] (reproduced).

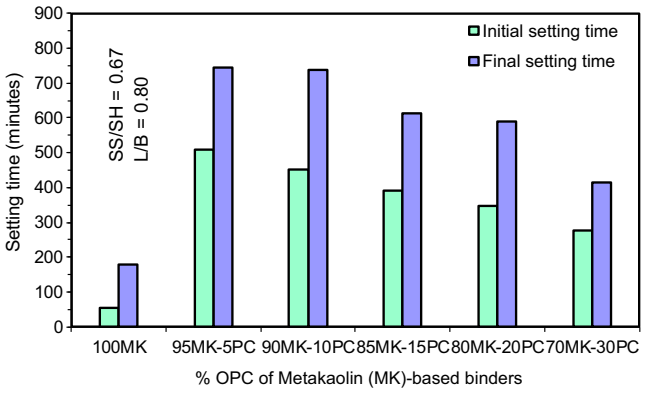

Fig. 14. Effect of OPC replacement on setting time of metakaolin-based alkaline binder [122] (reproduced).

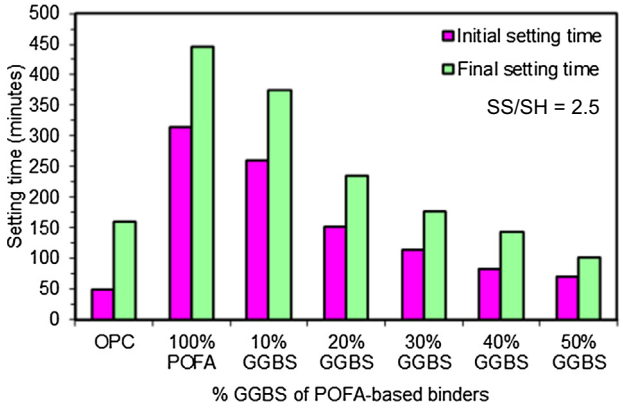

Fig. 15. Effect of slag content on setting time of POFA-based alkaline binder [111] (reproduced).

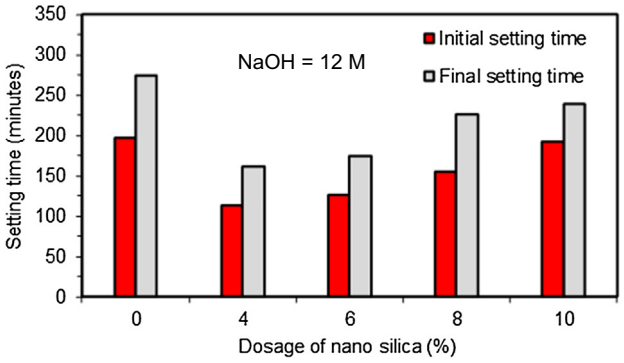

Fig. 16. Influence of nano silica on setting time of FA-based alkaline binder [203] (reproduced).

the hydration kinetics of alkaline binders [205,206]. The heat generated during the hydration reaction of AABs has been investigated in many studies [174,206–215]. Similar to OPC, chemically activated pozzolans exhibit four stages including initial dissolution, induction (dormant period), acceleration/deceleration and stable (steady state) period as reported in several investigations [213,214,216–221]. The effect of pozzolan types and proportion, solution modulus (molar ratio of SiO_2 to Na_2O), and temperature on the heat signature of fly ash/slag-based binders has been examined by Chithiraputhiran and Neithalath [222]. These authors observed comparatively higher heat release for fly ash-based paste than slag-based paste. In addition to this, the effect of slag proportion and activator types on very early age hydration kinetics of activated slag-based binder was also studied by Gebregziabiher et al. [217]. In this study, short and long induction period of AA slag paste was observed with NaOH and Na_2SiO_3 activators, respectively, and also a higher heat evolution was observed with increased dosage of NaOH [217]. Fig. 17 shows the isothermal calorimetry for OPC-GGBS alkali-activated systems. The first peak is correlated to the rapid dissolution of gypsum and calcium aluminates, initial hydration of alite (C_3S), and formation of ettringite (AFt) [213] while the second peak has been attributed to the formation of calcium silicate hydrate through silicate (C_2S and C_3S) hydration [217] in the activated slag-cement binder [214].

The OPC-GGBS (80%) mixture activated with NaOH and NaOH + Na_2SiO_3 significantly delayed reaction compared to this mixture activated with NaOH alone as shown in Fig. 17. This phenomenon is attributed to the increased alkalinity of the entire system, hence activating the slag, which was confirmed by other literature [214,216,218]. In contrast, higher heat flow and higher cumulative heat was found when slag content was added to a fly ash-based alkaline binder system [174]. The effect of molar concentration on the heat flow characteristics of activated slag was experimented in another study, which revealed that the heat flow and cumulative heat generation increase with increased molarity of NaOH [217].

The solution modulus (Ms), which is defined as the molar ratio of SiO_2 to Na_2O, can have a considerable effect on hydration reaction. In general, a lower MS results in higher cumulative heat. This was shown by Shearer, who found that the solution modulus had the largest impact on the magnitude and temporal occurrence of calorimetry peaks when reacting fly ash with both sodium and potassium-based activating solutions [223]. Additionally, an increase in temperature significantly accelerated the reaction rate

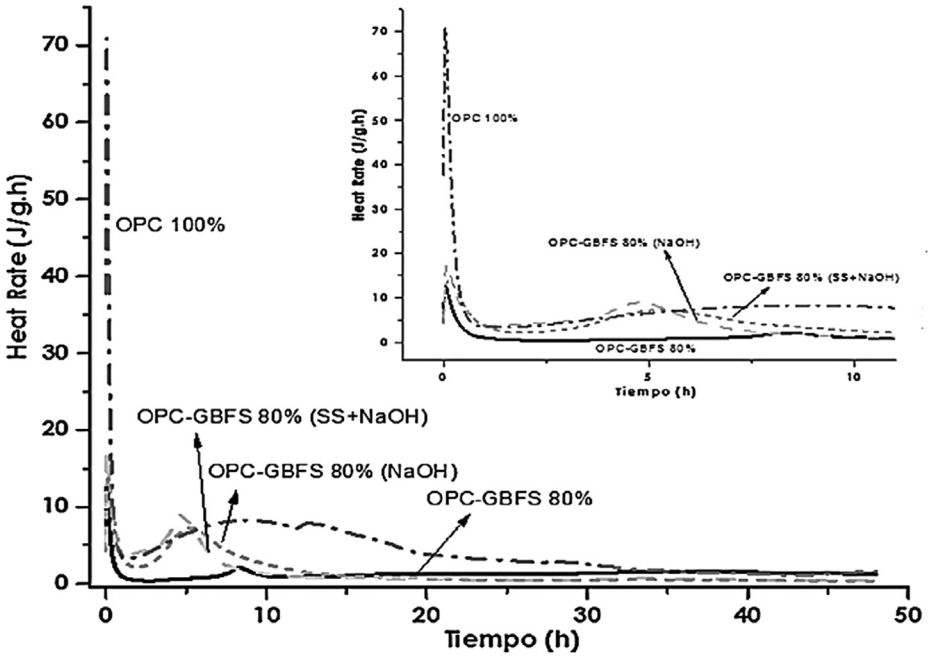

Fig. 17. Hydration kinetics of slag/OPC activated binders [214] (adapted).

and increased the cumulative heat released. Gebregziabiher et al., who studied the hydration heat phenomenon of slag-FA activated with different solution modulus values, also found this to be true as shown Fig. 18 [217]. Similarly, other studies have also revealed increased heat flow with decreased Ms [224,225]. The higher intensity heat signatures at lower Ms values was due to their higher alkalinity, which improved the solubility of silica and alumina of raw phosphorus slag and ultimately produced a greater reaction [226–228]. Gao et al. also examined the effect of a green olivine nano-silica based activator on AA slag-FA blends and reported delayed early age reaction with increased activator modulus [211].

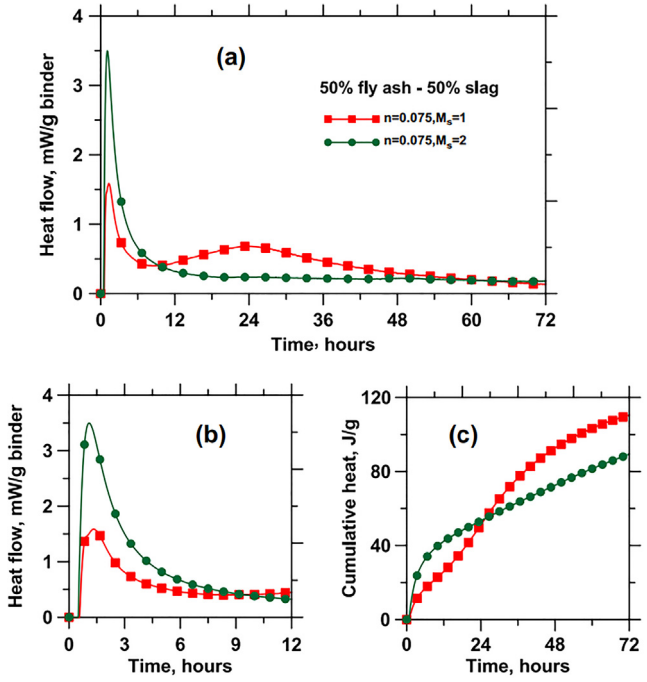

Fig. 18. Heat flow of slag-FA (a and b) and cumulative heat release (c) of slag-FA (50/50) alkaline binders [222] (adapted).

Xie et al. also reported that the lower Ms accelerated the heat flow and resulted in higher cumulative heat in an alkali-activated phosphorous slag system [210]. In this particular study, the initial dissolution peaks formed very early refer to the zoomed part of the Fig. 19.

3.5. Temperature of fresh alkali-activated concrete

The temperature of fresh alkali-activated concrete is an important parameter that influences placement, strength, and durability. In particular, the temperature of concrete is crucial during the placement in the field in extreme hot and/or cold weather. The difference between ambient temperature and the fresh concrete temperature should be within a specified range to ensure proper hydration, which dictates the strength and durability. Due to the exothermic reaction during geopolymerization, a higher temperature is produced in alkaline binder based concrete compared to the ambient temperature [95]. Jumrat et al. reported that the maximum temperature increase occurred after 1 h from mixing and

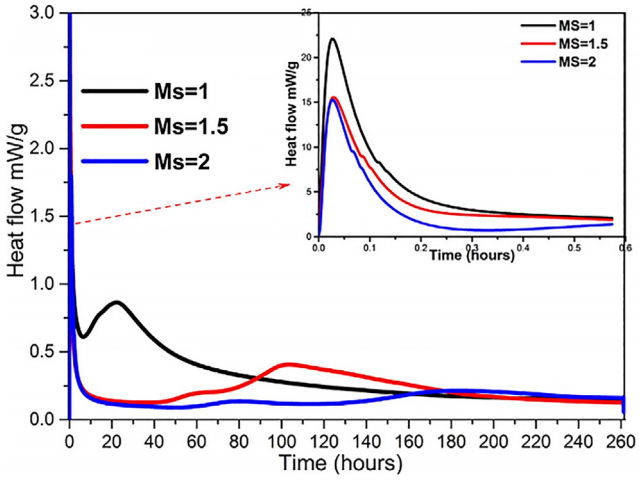

Fig. 19. Isothermal calorimetry curve for alkaline phosphate pastes with different Ms [210] (adapted).

drastically decreased after 3 h in fly ash-based alkaline mortar [176]. The change temperature was recorded resulting from different mixture variables including activator to fly ash ratio and fine aggregates to fly ash ratio as examined by Kotwal et al. [177]. This study stated that the temperature increased with increased sodium silicate and sodium hydroxide concentration and decreased with increased proportion of fine aggregates. The temperature of AA fly ash-based concrete was in a range from 32 to 54 °C as reported in another study [229].

4. Conclusions

Based on the published literature related to the material composition and fresh properties of alkali-activated concrete, the following conclusions can be drawn:

(i) A wide variety of industrial and agricultural by-products and other waste materials studied as a source of aluminosilicate and calcium have been categorized in terms of physical, chemical, and morphological properties. These properties directly affect the fresh properties of alkali-activated binders.
(ii) The oxide composition of pozzolans has a significant influence on the fresh properties of AAB. The proportion of silica and calcium in raw pozzolans controls different parameters of the fresh concrete prepared with alkaline binders.
(iii) The fresh properties of AAB made with different pozzolans such as slag, FA, RHA, POFA, and metakaolin using different activators were studied and compared based on the type of precursor and alkali activators. Workability and setting time tend to decrease when high calcium materials such as GGBS and OPC are added to the mixture. This has been attributed to accelerated hydration.
(iv) The composition of the alkali activator and its molar concentration has a significant impact on the workability and setting time of AAB concrete because of changes in viscosity and alkalinity of the solution. Workability of fly ash and slag-based alkali-activated binders decreases with increased molar ratio of sodium silicate to sodium hydroxide. Setting time has been shown to decrease with increased molarity of alkaline solution.
(v) The heat of hydration of AAB depends on the type and concentration of activators, solution modulus, and pozzolan type. An increase in molarity of NaOH increases the heat flow and cumulative heat and the addition of sodium silicate to sodium hydroxide delays the reaction compared to sodium hydroxide alone. In addition, a lower solution modulus generates higher cumulative heat in general. Alkali activated slags and fly ash with and without OPC have significantly different reaction kinetics.
(vi) The temperature of concrete made with AAB is influenced by the same parameters as heat of hydration with increased temperature observed after reaction compared to ambient.

Declaration of Competing Interest

The authors declare that they have no known competing financial interests or personal relationships that could have appeared to influence the work reported in this paper.

Acknowledgements

This study was funded by the first author's current employer named Intertek USA, Inc, 3730 Dacoma St, Houston, TX 77092 United States under the Technical Paper Incentive Program (SOP TR-11). All opinions expressed in this article are the author's and do not necessarily reflect the policies of Intertek USA, Inc. The second, third, and fourth author acknowledge the financial and technical supports provided by their respective affiliated organisations. The fifth author provided a tremendous support to evaluate the technical aspects of this article and shows his gratitude to South Dakota School of Mines & Technology.

References

[1] Y.J. Patel, N. Shah, Enhancement of the properties of ground granulated blast furnace slag based self compacting geopolymer concrete by incorporating rice husk ash, Constr. Build. Mater. 171 (2018) 654–662.
[2] E. Aprianti et al., Supplementary cementitious materials origin from agricultural wastes–A review, Constr. Build. Mater. 74 (2015) 176–187.
[3] J.S. Damtoft et al., Sustainable development and climate change initiatives, Cem. Concr. Res. 38 (2) (2008) 115–127.
[4] L. Prasittisopin, D. Trejo, Hydration and phase formation of blended cementitious systems incorporating chemically transformed rice husk ash, Cem. Concr. Compos. 59 (2015) 100–106.
[5] H. Scharff, Landfill reduction experience in The Netherlands, Waste Manage. 34 (11) (2014) 2218–2224.
[6] K.H. Yang, J.K. Song, K.I. Song, Assessment of CO_2 reduction of alkali-activated concrete, J. Cleaner Prod. 39 (2013) 265–272.
[7] Davidovits, J., Geopolymer chemistry and applications. 2008: Geopolymer Institute.
[8] P. Duxson et al., Geopolymer technology: the current state of the art, J. Mater. Sci. 42 (9) (2007) 2917–2933.
[9] P. Duxson et al., The role of inorganic polymer technology in the development of green concrete, Cem. Concr. Res. 37 (12) (2007) 1590–1597.
[10] P. Chindaprasirt, T. Chareerat, V. Sirivivatnanon, Workability and strength of coarse high calcium fly ash geopolymer, Cem. Concr. Compos. 29 (3) (2007) 224–229.
[11] X. Guo, H. Shi, W.A. Dick, Compressive strength and microstructural characteristics of class C fly ash geopolymer, Cem. Concr. Compos. 32 (2) (2010) 142–147.
[12] M.R. Karim et al., Effects of source materials, fineness and curing methods on the strength development of alkali-activated binder, J. Build. Eng. 29 (2020) 101147.
[13] W.K.W. Lee, J.S.J. van Deventer, The effect of ionic contaminants on the early-age properties of alkali-activated fly ash-based cements, Cem. Concr. Res. 32 (4) (2002) 577–584.
[14] Lee, N., J. Jagn, and H.K. Lee. Effect of blast furnace slag on drying shrinkage of fly ash-based paste and mortar activated with sodium silicate. The 5th International Conference of Asian Concrete Federation. 2012.
[15] P. Duxson, G.C. Lukey, J.S.J. van Deventer, Thermal conductivity of metakaolin geopolymers used as a first approximation for determining gel interconnectivity, Ind. Eng. Chem. Res. 45 (23) (2006) 7781–7788.
[16] P.M. Gifford, J.E. Gillott, Freeze-thaw durability of activated blast furnace slag cement concrete, Mater. J. 93 (3) (1996) 242–245.
[17] I. García-Lodeiro, A. Palomo, A. Fernández-Jiménez, Alkali–aggregate reaction in activated fly ash systems, Cem. Concr. Res. 37 (2) (2007) 175–183.
[18] V. Sata, A. Sathonsaowaphak, P. Chindaprasirt, Resistance of lignite bottom ash geopolymer mortar to sulfate and sulfuric acid attack, Cem. Concr. Compos. 34 (5) (2012) 700–708.
[19] F. Škvára, T. Jílek, L. Kopecký, Geopolymer materials based on fly ash, Ceram.-Silik 49 (3) (2005) 195–204.
[20] M.M. Hossain et al., Long-term durability properties of alkali-activated binders containing slag, fly ash, palm oil fuel ash and rice husk ash, Constr. Build. Mater. 251 (2020) 119094.
[21] M.M. Hossain et al., Water absorption and sorptivity of alkali-activated ternary blended composite binder, J. Build. Eng. 31 (2020) 101370.
[22] C. Shi, A.F. Jiménez, A. Palomo, New cements for the 21st century: the pursuit of an alternative to Portland cement, Cem. Concr. Res. 41 (7) (2011) 750–763.
[23] K.H. Yang et al., Tests on cementless alkali-activated slag concrete using lightweight aggregates, Int. J. Concr. Struct. Mater. 5 (2) (2011) 125–131.
[24] F. Puertas et al., Alkali-activated fly ash/slag cements: Strength behaviour and hydration products, Cem. Concr. Res. 30 (10) (2000) 1625–1632.
[25] A. Katz, Microscopic study of alkali-activated fly ash, Cem. Concr. Res. 28 (2) (1998) 197–208.
[26] H. Wang, H. Li, F. Yan, Synthesis and mechanical properties of metakaolinite-based geopolymer, Colloids Surf., A 268 (1–3) (2005) 1–6.
[27] A. Palomo, M. Grutzeck, M. Blanco, Alkali-activated fly ashes: a cement for the future, Cem. Concr. Res. 29 (8) (1999) 1323–1329.
[28] C.R. Shearer et al., Alkali-activation potential of biomass-coal co-fired fly ash, Cem. Concr. Compos. 73 (2016) 62–74.
[29] S.D. Wang, K.L. Scrivener, P.L. Pratt, Factors affecting the strength of alkali-activated slag, Cem. Concr. Res. 24 (6) (1994) 1033–1043.
[30] M. Criado, A. Palomo, A. Fernández-Jiménez, Alkali activation of fly ashes. Part 1: effect of curing conditions on the carbonation of the reaction products, Fuel 84 (16) (2005) 2048–2054.

[31] A. Fernández-Jiménez, A. Palomo, Characterisation of fly ashes. Potential reactivity as alkaline cements☆, Fuel 82 (18) (2003) 2259–2265.
[32] A. Fernández-Jiménez, A. Palomo, Composition and microstructure of alkali activated fly ash binder: effect of the activator, Cem. Concr. Res. 35 (10) (2005) 1984–1992.
[33] D. Hardjito et al., Properties of geopolymer concrete with fly ash as source material: effect of mixture composition, Spec. Publ. 222 (2004) 109–118.
[34] A.A. Adam, X.X.X. Horianto, The effect of temperature and duration of curing on the strength of fly ash based geopolymer mortar, Procedia Eng. 95 (2014) 410–414.
[35] A.M. Al Bakri et al., The processing, characterization, and properties of fly ash based geopolymer concrete, Rev. Adv. Mater. Sci. 30 (1) (2012) 90–97.
[36] F. Collins, J. Sanjayan, Development of novel alkali activated slag binders to achieve high early strength concrete for construction use, Austr. Civil Eng. Trans. 44 (2002) 91.
[37] R. Firdous, D. Stephan, J.N.Y. Djobo, Natural pozzolan based geopolymers: a review on mechanical, microstructural and durability characteristics, Constr. Build. Mater. 190 (2018) 1251–1263.
[38] J. Newman, B.S. Choo, Advanced Concrete Technology Set, Elsevier, 2003.
[39] B. Sharif, R. Firdous, M.A. Tahir, Development of local bagasse ash as pozzolanic material for use in concrete, Pak. J. Eng. Appl. Sci. 17 (2015) 39–45.
[40] J. Dietel et al., The importance of specific surface area in the geopolymerization of heated illitic clay, Appl. Clay Sci. 139 (2017) 99–107.
[41] M.L. Gualtieri et al., Inorganic polymers from laterite using activation with phosphoric acid and alkaline sodium silicate solution: mechanical and microstructural properties, Cem. Concr. Res. 67 (2015) 259–270.
[42] R. Kaze et al., The corrosion of kaolinite by iron minerals and the effects on geopolymerization, Appl. Clay Sci. 138 (2017) 48–62.
[43] L. Valentini et al., Alkali-activated calcined smectite clay blended with waste calcium carbonate as a low-carbon binder, J. Cleaner Prod. 184 (2018) 41–49.
[44] S. Ahmari, L. Zhang, Utilization of cement kiln dust (CKD) to enhance mine tailings-based geopolymer bricks, Constr. Build. Mater. 40 (2013) 1002–1011.
[45] L. Zhang, S. Ahmari, J. Zhang, Synthesis and characterization of fly ash modified mine tailings-based geopolymers, Constr. Build. Mater. 25 (9) (2011) 3773–3781.
[46] M. Zhang et al., Synthesis factors affecting mechanical properties, microstructure, and chemical composition of red mud–fly ash based geopolymers, Fuel 134 (2014) 315–325.
[47] J. He et al., The strength and microstructure of two geopolymers derived from metakaolin and red mud-fly ash admixture: a comparative study, Constr. Build. Mater. 30 (2012) 80–91.
[48] A. Kumar, S. Kumar, Development of paving blocks from synergistic use of red mud and fly ash using geopolymerization, Constr. Build. Mater. 38 (2013) 865–871.
[49] D.D. Dimas, I.P. Giannopoulou, D. Panias, Utilization of alumina red mud for synthesis of inorganic polymeric materials, Miner. Process. Extr. Metall. Rev. 30 (3) (2009) 211–239.
[50] N. Ye et al., Synthesis and strength optimization of one-part geopolymer based on red mud, Constr. Build. Mater. 111 (2016) 317–325.
[51] C. Bagci, G.P. Kutyla, W.M. Kriven, Fully reacted high strength geopolymer made with diatomite as a fumed silica alternative, Ceram. Int. 43 (17) (2017) 14784–14790.
[52] H. Tchakoute Kouamo et al., Synthesis of volcanic ash-based geopolymer mortars by fusion method: effects of adding metakaolin to fused volcanic ash, Ceram. Int. 39 (2) (2013) 1613–1621.
[53] A. Aziz et al., Effect of slaked lime on the geopolymers synthesis of natural pozzolan from Moroccan Middle Atlas, J. Aust. Ceram. Soc. 56 (1) (2020) 67–78.
[54] E. Najafi Kani, A. Allahverdi, J.L. Provis, Calorimetric study of geopolymer binders based on natural pozzolan, J. Therm. Anal. Calorim. 127 (3) (2017) 2181–2190.
[55] H.S. Hassan et al., Cleaner production of one-part white geopolymer cement using pre-treated wood biomass ash and diatomite, J. Cleaner Prod. 209 (2019) 1420–1428.
[56] A. Nana et al., Room-temperature alkaline activation of feldspathic solid solutions: development of high strength geopolymers, Constr. Build. Mater. 195 (2019) 258–268.
[57] Z. Zhang et al., Conversion of local industrial wastes into greener cement through geopolymer technology: a case study of high-magnesium nickel slag, J. Cleaner Prod. 141 (2017) 463–471.
[58] Y. Wu et al., Geopolymer, green alkali activated cementitious material: Synthesis, applications and challenges, Constr. Build. Mater. 224 (2019) 930–949.
[59] B. Nematollahi, J. Sanjayan, F.U.A. Shaikh, Synthesis of heat and ambient cured one-part geopolymer mixes with different grades of sodium silicate, Ceram. Int. 41 (4) (2015) 5696–5704.
[60] K.-T. Wang et al., Preparation of drying powder inorganic polymer cement based on alkali-activated slag technology, Powder Technol. 312 (2017) 204–209.
[61] K.-H. Yang, J.-K. Song, Workability loss and compressive strength development of cementless mortars activated by combination of sodium silicate and sodium hydroxide, J. Mater. Civ. Eng. 21 (3) (2009) 119–127.
[62] K.-H. Yang et al., Properties of cementless mortars activated by sodium silicate, Constr. Build. Mater. 22 (9) (2008) 1981–1989.
[63] P. Chindaprasirt et al., Effect of SiO2 and Al2O3 on the setting and hardening of high calcium fly ash-based geopolymer systems, J. Mater. Sci. 47 (12) (2012) 4876–4883.
[64] U. Rattanasak, K. Pankhet, P. Chindaprasirt, Effect of chemical admixtures on properties of high-calcium fly ash geopolymer, Int. J. Miner. Metall. Mater. 18 (3) (2011) 364.
[65] Duxson, P., 3 - Geopolymer precursor design, in Geopolymers, J.L. Provis and J. S.J. van Deventer, Editors. 2009, Woodhead Publishing. pp. 37–49.
[66] P. Duxson, J.L. Provis, Designing precursors for geopolymer cements, J. Am. Ceram. Soc. 91 (12) (2008) 3864–3869.
[67] S.A. Hasanein et al., Resistance of alkali activated water-cooled slag geopolymer to sulphate attack, Ceramics-Silikáty 55 (2) (2011) 153–160.
[68] J. He et al., Synthesis and characterization of red mud and rice husk ash-based geopolymer composites, Cem. Concr. Compos. 37 (2013) 108–118.
[69] G.F. Huseien et al., Effect of metakaolin replaced granulated blast furnace slag on fresh and early strength properties of geopolymer mortar, Ain Shams Eng. J. 9 (4) (2018) 1557–1566.
[70] G.A. Habeeb, H.B. Mahmud, Study on properties of rice husk ash and its use as cement replacement material, Mater. Res. 13 (2010) 185–190.
[71] S. Turmanova, S. Genieva, L. Vlaev, Obtaining some polymer composites filled with rice husks ash-a review, Int. J. Chem. 4 (4) (2012) 62.
[72] R. Pode, Potential applications of rice husk ash waste from rice husk biomass power plant, Renew. Sustain. Energy Rev. 53 (2016) 1468–1485.
[73] E. Foletto et al., Conversion of rice husk ash into zeolitic materials, Latin Am. Appl. Res. 39 (1) (2009) 75–78.
[74] S. Detphan, P. Chindaprasirt, Preparation of fly ash and rice husk ash geopolymer, Int. J. Miner. Metall. Mater. 16 (6) (2009) 720–726.
[75] A. Nazari, A. Bagheri, S. Riahi, Properties of geopolymer with seeded fly ash and rice husk bark ash, Mater. Sci. Eng. A 528 (24) (2011) 7395–7401.
[76] W. Tangchirapat, C. Jaturapitakkul, P. Chindaprasirt, Use of palm oil fuel ash as a supplementary cementitious material for producing high-strength concrete, Constr. Build. Mater. 23 (7) (2009) 2641–2646.
[77] H. Noorvand et al., Physical and chemical characteristics of unground palm oil fuel ash cement mortars with nanosilica, Constr. Build. Mater. 48 (2013) 1104–1113.
[78] M.M. Johari et al., Engineering and transport properties of high-strength green concrete containing high volume of ultrafine palm oil fuel ash, Constr. Build. Mater. 30 (2012) 281–288.
[79] M.O. Yusuf et al., Strength and microstructure of alkali-activated binary blended binder containing palm oil fuel ash and ground blast-furnace slag, Constr. Build. Mater. 52 (2014) 504–510.
[80] Yusuf, M.O., et al., Effects of H2O/Na2O molar ratio on the strength of alkaline activated ground blast furnace slag-ultrafine palm oil fuel ash based concrete. Materials & Design (1980-2015), 2014. 56: p. 158-164.
[81] Islam, A., et al., The development of compressive strength of ground granulated blast furnace slag-palm oil fuel ash-fly ash based geopolymer mortar. Materials & Design (1980-2015), 2014. 56: p. 833-841.
[82] M.R. Karim et al., Fabrication of a non-cement binder using slag, palm oil fuel ash and rice husk ash with sodium hydroxide, Constr. Build. Mater. 49 (2013) 894–902.
[83] M.J.A. Mijarsh, M.A. Megat Johari, Z.A. Ahmad, Synthesis of geopolymer from large amounts of treated palm oil fuel ash: application of the Taguchi method in investigating the main parameters affecting compressive strength, Constr. Build. Mater. 52 (2014) 473–481.
[84] E. Kamseu et al., Design of inorganic polymer cements: effects of matrix strengthening on microstructure, Constr. Build. Mater. 38 (2013) 1135–1145.
[85] Z. Li et al., Chemical deformation of metakaolin based geopolymer, Cem. Concr. Res. 120 (2019) 108–118.
[86] K.T. Wang et al., Effects of the metakaolin-based geopolymer on high-temperature performances of geopolymer/PVC composite materials, Appl. Clay Sci. 114 (2015) 586–592.
[87] A.M. Rashad, Metakaolin: fresh properties and optimum content for mechanical strength in traditional cementitious materials—a comprehensive overview, Rev. Adv. Mater. Sci 40 (1) (2015) 15–44.
[88] G. Kakali et al., Thermal treatment of kaolin: the effect of mineralogy on the pozzolanic activity, Appl. Clay Sci. 20 (1–2) (2001) 73–80.
[89] A. Ito, R. Wagai, Global distribution of clay-size minerals on land surface for biogeochemical and climatological studies, Sci. Data 4 (2017) 170103.
[90] K.L. Scrivener, Options for the future of cement, Indian Concr. J 88 (7) (2014) 11–21.
[91] Sindhunata et al., Effect of curing temperature and silicate concentration on fly-ash-based geopolymerization, Ind. Eng. Chem. Res. 45 (10) (2006) 3559–3568.
[92] Provis, J.L. and J.S. Van Deventer, Alkali activated materials: state-of-the-art report, RILEM TC 224-AAM. Vol. 13. 2013: Springer Science & Business Media.
[93] A. Palomo et al., Chemical stability of cementitious materials based on metakaolin, Cem. Concr. Res. 29 (7) (1999) 997–1004.
[94] A. Shalini, G. Gurunarayanan, S. Sakthivel, Performance of rice husk ash in geopolymer concrete, Int. J. Innov Res. Sci. Technol. 2 (2016) 73–77.
[95] J. Davidovits, Geopolymers: inorganic polymeric new materials, J. Therm. Anal. Calorim. 37 (8) (1991) 1633–1656.
[96] C. Madheswaran, G. Gnanasundar, N. Gopalakrishnan, Effect of molarity in geopolymer concrete, Int. J. Civil Struct. Eng. 4 (2) (2013) 106.
[97] Davidovits, J. Properties of geopolymer cements. in First international conference on alkaline cements and concretes. 1994. Scientific Research Institute on Binders and Materials Kiev, Ukraine.
[98] K. Somna et al., NaOH-activated ground fly ash geopolymer cured at ambient temperature, Fuel 90 (6) (2011) 2118–2124.

[99] A. Hajimohammadi, J.S. van Deventer, Characterisation of one-part geopolymer binders made from fly ash, Waste Biomass Valorization 8 (1) (2017) 225–233.
[100] B. Nematollahi et al., Micromechanics-based investigation of a sustainable ambient temperature cured one-part strain hardening geopolymer composite, Constr. Build. Mater. 131 (2017) 552–563.
[101] M.H. Al-Majidi et al., Development of geopolymer mortar under ambient temperature for in situ applications, Constr. Build. Mater. 120 (2016) 198–211.
[102] H.Y. Zhang et al., Characterizing the bond strength of geopolymers at ambient and elevated temperatures, Cem. Concr. Compos. 58 (2015) 40–49.
[103] M.R. Karim et al., Development of a zero-cement binder using slag, fly ash, and rice husk ash with chemical activator, Adv. Mater. Sci. Eng. 2015 (2015) 247065.
[104] C. Atiş et al., Very high strength (120 MPa) class F fly ash geopolymer mortar activated at different NaOH amount, heat curing temperature and heat curing duration, Constr. Build. Mater. 96 (2015) 673–678.
[105] V. Živica, M.T. Palou, M. Križma, Geopolymer cements and their properties: a review, Build. Res. J. 61 (2) (2015) 85–100.
[106] Provis, J. and S.A. Bernal, Performance of sodium carbonate/silicate activated slag materials. International Conference on Alkali Activated Materials and Geopolymers: Versatile Materials Offering High Performance and Low Emmisions. 2018. Tomar Portugal.
[107] H. Choo et al., Compressive strength of one-part alkali activated fly ash using red mud as alkali supplier, Constr. Build. Mater. 125 (2016) 21–28.
[108] C. Li, H. Sun, L. Li, A review: the comparison between alkali-activated slag (Si+ Ca) and metakaolin (Si+ Al) cements, Cem. Concr. Res. 40 (9) (2010) 1341–1349.
[109] M.S. Kim et al., Use of CaO as an activator for producing a price-competitive non-cement structural binder using ground granulated blast furnace slag, Cem. Concr. Res. 54 (2013) 208–214.
[110] M. Ismail, M.E. Ismail, B. Muhammad, Influence of elevated temperatures on physical and compressive strength properties of concrete containing palm oil fuel ash, Constr. Build. Mater. 25 (5) (2011) 2358–2364.
[111] M.A. Salih et al., Development of high strength alkali activated binder using palm oil fuel ash and GGBS at ambient temperature, Constr. Build. Mater. 93 (2015) 289–300.
[112] A. Sharmin et al., Influence of source materials and the role of oxide composition on the performance of ternary blended sustainable geopolymer mortar, Constr. Build. Mater. 144 (2017) 608–623.
[113] A. Mehta, R. Siddique, Sustainable geopolymer concrete using ground granulated blast furnace slag and rice husk ash: strength and permeability properties, J. Cleaner Prod. 205 (2018) 49–57.
[114] J. Xie et al., Effects of combined usage of GGBS and fly ash on workability and mechanical properties of alkali activated geopolymer concrete with recycled aggregate, Compos. B Eng. 164 (2019) 179–190.
[115] A. Kusbiantoro et al., The effect of microwave incinerated rice husk ash on the compressive and bond strength of fly ash based geopolymer concrete, Constr. Build. Mater. 36 (2012) 695–703.
[116] E. Nimwinya et al., A sustainable calcined water treatment sludge and rice husk ash geopolymer, J. Cleaner Prod. 119 (2016) 128–134.
[117] N. Ranjbar et al., Compressive strength and microstructural analysis of fly ash/palm oil fuel ash based geopolymer mortar, Mater. Des. 59 (2014) 532–539.
[118] A.A. Awal, M.W. Hussin, Effect of palm oil fuel ash in controlling heat of hydration of concrete, Procedia Eng. 14 (2011) 2650–2657.
[119] P. Pavithra et al., A mix design procedure for geopolymer concrete with fly ash, J. Cleaner Prod. 133 (2016) 117–125.
[120] D. Adak, M. Sarkar, S. Mandal, Structural performance of nano-silica modified fly-ash based geopolymer concrete, Constr. Build. Mater. 135 (2017) 430–439.
[121] S. Zeng, J. Wang, Characterization of mechanical and electric properties of geopolymers synthesized using four locally available fly ashes, Constr. Build. Mater. 121 (2016) 386–399.
[122] K. Wianglor et al., Effect of alkali-activated metakaolin cement on compressive strength of mortars, Appl. Clay Sci. 141 (2017) 272–279.
[123] S. Jena, R. Panigrahi, P. Sahu, Effect of Silica Fume on the Properties of Fly Ash Geopolymer Concrete, in Sustainable, Constr. Build. Mater. (2019) 145–153. Springer.
[124] H.M. Hamada et al., Fresh and hardened properties of palm oil clinker lightweight aggregate concrete incorporating Nano-palm oil fuel ash, Constr. Build. Mater. 214 (2019) 344–354.
[125] T. Tho-In et al., Compressive strength and microstructure analysis of geopolymer paste using waste glass powder and fly ash, J. Cleaner Prod. 172 (2018) 2892–2898.
[126] G.F. Huseien et al., Properties of ceramic tile waste based alkali-activated mortars incorporating GBFS and fly ash, Constr. Build. Mater. 214 (2019) 355–368.
[127] P.H. Borges et al., Performance of blended metakaolin/blastfurnace slag alkali-activated mortars, Cem. Concr. Compos. 71 (2016) 42–52.
[128] D. Huiskes et al., Design and performance evaluation of ultra-lightweight geopolymer concrete, Mater. Des. 89 (2016) 516–526.
[129] D.L. Kong, J.G. Sanjayan, Effect of elevated temperatures on geopolymer paste, mortar and concrete, Cem. Concr. Res. 40 (2) (2010) 334–339.
[130] N. Nadziri, I. Ismail, S. Hamdan, Binding gel characterization of alkali-activated binders based on palm oil fuel ash (POFA) and fly ash, J. Sustain. Cem. Based Mater. 7 (1) (2018) 1–14.
[131] O.A. Abdulkareem et al., Effects of elevated temperatures on the thermal behavior and mechanical performance of fly ash geopolymer paste, mortar and lightweight concrete, Constr. Build. Mater. 50 (2014) 377–387.
[132] P. Duan et al., Effects of adding nano-TiO2 on compressive strength, drying shrinkage, carbonation and microstructure of fluidized bed fly ash based geopolymer paste, Constr. Build. Mater. 106 (2016) 115–125.
[133] N. Ranjbar et al., Compressive strength and microstructural analysis of fly ash/palm oil fuel ash based geopolymer mortar under elevated temperatures, Constr. Build. Mater. 65 (2014) 114–121.
[134] M.Y.J. Liu et al., Microstructural investigations of palm oil fuel ash and fly ash based binders in lightweight aggregate foamed geopolymer concrete, Constr. Build. Mater. 120 (2016) 112–122.
[135] B. Yan, P. Duan, D. Ren, Mechanical strength, surface abrasion resistance and microstructure of fly ash-metakaolin-sepiolite geopolymer composites, Ceram. Int. 43 (1) (2017) 1052–1060.
[136] R.A.A.B. Santa, C. Soares, H.G. Riella, Geopolymers obtained from bottom ash as source of aluminosilicate cured at room temperature, Constr. Build. Mater. 157 (2017) 459–466.
[137] T. Xie, T. Ozbakkaloglu, Behavior of low-calcium fly and bottom ash-based geopolymer concrete cured at ambient temperature, Ceram. Int. 41 (4) (2015) 5945–5958.
[138] ASTM C618-19, Standard Specification for Coal Fly Ash and Raw or Calcined Natural Pozzolan for Use in Concrete in ASTM International. 2019, ASTM International: West Conshohocken, PA.
[139] N. Xie et al., Upcycling of waste materials: Green binder prepared with pure coal fly ash, J. Mater. Civ. Eng. 28 (3) (2015) 04015138.
[140] G. Xu, X. Shi, Exploratory investigation into a chemically activated fly ash binder for mortars, J. Mater. Civ. Eng. 29 (11) (2017) 06017018.
[141] P. Chindaprasirt, S. Rukzon, V. Sirivivatnanon, Resistance to chloride penetration of blended Portland cement mortar containing palm oil fuel ash, rice husk ash and fly ash, Constr. Build. Mater. 22 (5) (2008) 932–938.
[142] F. Okoye, J. Durgaprasad, N. Singh, Effect of silica fume on the mechanical properties of fly ash based-geopolymer concrete, Ceram. Int. 42 (2) (2016) 3000–3006.
[143] L. Assi et al., Improvement of the early and final compressive strength of fly ash-based geopolymer concrete at ambient conditions, Constr. Build. Mater. 123 (2016) 806–813.
[144] N. Marjanović et al., Physical–mechanical and microstructural properties of alkali-activated fly ash–blast furnace slag blends, Ceram. Int. 41 (1) (2015) 1421–1435.
[145] H. Alanazi, J. Hu, Y.-R. Kim, Effect of slag, silica fume, and metakaolin on properties and performance of alkali-activated fly ash cured at ambient temperature, Constr. Build. Mater. 197 (2019) 747–756.
[146] T. Kovářík et al., Thermomechanical properties of particle-reinforced geopolymer composite with various aggregate gradation of fine ceramic filler, Constr. Build. Mater. 143 (2017) 599–606.
[147] M.H. Samarakoon et al., Recent advances in alkaline cement binders: a review, J. Cleaner Prod. 227 (2019) 70–87.
[148] D. Singhal et al., Mechanical and microstructural properties of fly ash based geopolymer concrete incorporating alccofine at ambient curing, Constr. Build. Mater. 180 (2018) 298–307.
[149] B.B. Jindal et al., Enhancing mechanical and durability properties of geopolymer concrete with mineral admixture, Comput. Concr. 21 (3) (2018) 345–353.
[150] R. Terzano et al., Characterization of different coal fly ashes for their application in the synthesis of zeolite X as cation exchanger for soil remediation, Fresenius Environ. Bull. 14 (4) (2005) 263–267.
[151] B.B. Jindal, Feasibility study of ambient cured geopolymer concrete-A review, Adv. Concr. Constr. 6 (4) (2018) 387–405.
[152] G.F. Huseien et al., Effect of metakaolin replaced granulated blast furnace slag on fresh and early strength properties of geopolymer mortar, Ain Shams Eng. J. 9 (4) (2016) 1557–1566.
[153] H. Wan, Z. Shui, Z. Lin, Analysis of geometric characteristics of GGBS particles and their influences on cement properties, Cem. Concr. Res. 34 (1) (2004) 133–137.
[154] M. Dri, A. Sanna, M.M. Maroto-Valer, Mineral carbonation from metal wastes: effect of solid to liquid ratio on the efficiency and characterization of carbonated products, Appl. Energy 113 (2014) 515–523.
[155] Kim, Y.Y., et al., Strength and durability performance of alkali-activated rice husk ash geopolymer mortar. The Scientific World Journal, 2014. Article # 209584.
[156] D. Singhal, B.B. Jindal, Experimental study on geopolymer concrete prepared using high-silica RHA incorporating alccofine, Adv. Concr. Constr. 5 (4) (2017) 345.
[157] P. Parveen et al., Mechanical and microstructural study of rice husk ash geopolymer paste with ultrafine slag, Adv. Concr. Constr. 8 (3) (2019) 217–223.
[158] P. Chindaprasirt, C. Chotetanorm, S. Rukzon, Use of palm oil fuel ash to improve chloride and corrosion resistance of high-strength and high-workability concrete, J. Mater. Civ. Eng. 23 (4) (2010) 499–503.
[159] W. Tangchirapat et al., Use of waste ash from palm oil industry in concrete, Waste Manage. 27 (1) (2007) 81–88.
[160] C. Jaturapitakkul et al., Filler effect and pozzolanic reaction of ground palm oil fuel ash, Constr. Build. Mater. 25 (11) (2011) 4287–4293.

[161] C. Chandara et al., The effect of unburned carbon in palm oil fuel ash on fluidity of cement pastes containing superplasticizer, Constr. Build. Mater. 24 (9) (2010) 1590–1593.
[162] T. Sinsiri et al., Assessing the effect of biomass ashes with different finenesses on the compressive strength of blended cement paste, Mater. Des. 42 (2012) 424–433.
[163] S. Chatterji, N. Thaulow, P. Christensen, Puzzolanic activity of byproduct silica-fume from ferro-silicom production, Cem. Concr. Res. 12 (6) (1982) 781–784.
[164] K. Wi et al., Effect of using micropalm oil fuel ash as partial replacement of cement on the properties of cement mortar, Adv. Mater. Sci. Eng. 2018 (2018) 5164030.
[165] H. Paiva et al., Effect of pozzolans with different physical and chemical characteristics on concrete properties, Mater. Constr. 66 (322) (2016) 083.
[166] A. Fernández-Jiménez et al., Alkaline activation of metakaolin–fly ash mixtures: obtain of zeoceramics and zeocements, Microporous Mesoporous Mater. 108 (1–3) (2008) 41–49.
[167] K. Ganesan, K. Rajagopal, K. Thangavel, Rice husk ash blended cement: assessment of optimal level of replacement for strength and permeability properties of concrete, Constr. Build. Mater. 22 (8) (2008) 1675–1683.
[168] J. Phair, J. Van Deventer, Effect of silicate activator pH on the leaching and material characteristics of waste-based inorganic polymers, Miner. Eng. 14 (3) (2001) 289–304.
[169] E.D. Rodríguez et al., Effect of nanosilica-based activators on the performance of an alkali-activated fly ash binder, Cem. Concr. Compos. 35 (1) (2013) 1–11.
[170] S.F. Ahmad, Z. Shaikh, P. Naik, Portland-pozzolana Cement from Sugarcane Bagasse Ash; KVIC Technology in the Production of Lime and Alternative Cements in India, in Lime and Other Alternative Cements, Practical Action Publishing, 1992, pp. 172–186.
[171] P. Nath, P.K. Sarker, Effect of GGBFS on setting, workability and early strength properties of fly ash geopolymer concrete cured in ambient condition, Constr. Build. Mater. 66 (2014) 163–171.
[172] M.Z.N. Khan, Y. Hao, H. Hao, Synthesis of high strength ambient cured geopolymer composite by using low calcium fly ash, Constr. Build. Mater. 125 (2016) 809–820.
[173] S.H. Kosmatka, B. Kerkhoff, W.C. Panarese, Design and Control of Concrete Mixtures, Vol. 5420, Portland Cement Association Skokie, IL, 2002.
[174] M. Nedeljković, Z. Li, G. Ye, Setting, strength, and autogenous shrinkage of alkali-activated fly ash and slag pastes: Effect of slag content, Materials 11 (11) (2018) 2121.
[175] R. Siddique, M.I. Khan, Supplementary Cementing Materials, Springer Science & Business Media, 2011.
[176] S. Jumrat, B. Chatveera, P. Rattanadecho, Dielectric properties and temperature profile of fly ash-based geopolymer mortar, Int. Commun. Heat Mass Transfer 38 (2) (2011) 242–248.
[177] A.R. Kotwal et al., Characterization and early age physical properties of ambient cured geopolymer mortar based on class C fly ash, Int. J. Concr. Struct. Mater. 9 (1) (2015) 35–43.
[178] A. Bhowmick, S. Ghosh, Effect of synthesizing parameters on workability and compressive strength of fly ash based geopolymer mortar, Int. J. Civ. Struct. Eng. 3 (1) (2012) 168–177.
[179] G.F. Huseien et al., Influence of different curing temperatures and alkali activators on properties of GBFS geopolymer mortars containing fly ash and palm-oil fuel ash, Constr. Build. Mater. 125 (2016) 1229–1240.
[180] Malkawi, A.B., et al., Effects of alkaline solution on properties of the HCFA geopolymer mortars. Procedia Engineering, 2016. 148: p. 710-717 %@ 1877-7058.
[181] A. Sathonsaowaphak, P. Chindaprasirt, K. Pimraksa, Workability and strength of lignite bottom ash geopolymer mortar, J. Hazard. Mater. 168 (1) (2009) 44–50.
[182] P. Nath, P.K. Sarker, Use of OPC to improve setting and early strength properties of low calcium fly ash geopolymer concrete cured at room temperature, Cem. Concr. Compos. 55 (2015) 205–214.
[183] S. Pangdaeng et al., Influence of curing conditions on properties of high calcium fly ash geopolymer containing Portland cement as additive, Mater. Des. 53 (2014) 269–274.
[184] J.-X. Lu, C.S. Poon, Use of waste glass in alkali activated cement mortar, Constr. Build. Mater. 160 (2018) 399–407.
[185] B. Nematollahi, J. Sanjayan, Effect of different superplasticizers and activator combinations on workability and strength of fly ash based geopolymer, Mater. Des. 57 (2014) 667–672.
[186] P.S. Deb, P.K. Sarker, Effects of ultrafine fly ash on setting, strength, and porosity of geopolymers cured at room temperature, J. Mater. Civ. Eng. 29 (2) (2016) 06016021.
[187] C.-C. Hung, J.-J. Chang, The influence of mixture variables for the alkali-activated slag concrete on the properties of concrete, J. Mar. Sci. Technol. 21 (3) (2013) 229–237.
[188] S.M. Laskar, S. Talukdar, Preparation and tests for workability, compressive and bond strength of ultra-fine slag based geopolymer as concrete repairing agent, Constr. Build. Mater. 154 (2017) 176–190.
[189] T. Chareerat, P. Chindaprasirt, V. Sirivivatnanon, Workability and strength of coarse high calcium fly ash geopolymers, Cem. Concr. Composites 29 (2007) 224–229.
[190] Saloma, et al., Geopolymer Mortar with Fly Ash. MATEC Web Conf., 2016. 78: p. 01026 %U https://doi.org/10.1051/matecconf/20167801026.
[191] Rouyer, J. and A. Poulesquen, Evidence of a fractal percolating network during geopolymerization. Journal of the American Ceramic Society, 2015. 98(5): pp. 1580-1587 %@ 0002-7820.
[192] Musaddiq Laskar, S. and S. Talukdar, Development of ultrafine slag-based geopolymer mortar for use as repairing mortar. Journal of Materials in Civil Engineering, 2016. 29(5): p. 04016292 %@ 0899-1561.
[193] Phoo-ngernkham, T., et al., Compressive strength, bending and fracture characteristics of high calcium fly ash geopolymer mortar containing portland cement cured at ambient temperature. Arabian Journal for Science and Engineering, 2016. 41(4): p. 1263-1271 %@ 1319-8025.
[194] C. Shi, B. Qu, J.L. Provis, Recent progress in low-carbon binders, Cem. Concr. Res. 122 (2019) 227–250.
[195] Li, N., C. Shi, and Z. Zhang. A study on the setting characteristics of alkali-activated slag cement. in The 3rd International Conference on Chemical Activated Materials, Gold Coast, Australia. 2017.
[196] Li, N., et al. Some Progresses in the Challenges for Geopolymer. in IOP Conference Series: Materials Science and Engineering. 2018. IOP Publishing.
[197] Deb, P.S., P. Nath, and P.K. Sarker, The effects of ground granulated blast-furnace slag blending with fly ash and activator content on the workability and strength properties of geopolymer concrete cured at ambient temperature. Materials & Design (1980-2015), 2014. 62: pp. 32-39.
[198] G. Fang et al., Workability and mechanical properties of alkali-activated fly ash-slag concrete cured at ambient temperature, Constr. Build. Mater. 172 (2018) 476–487.
[199] S. Kumar, R. Kumar, S. Mehrotra, Influence of granulated blast furnace slag on the reaction, structure and properties of fly ash based geopolymer, J. Mater. Sci. 45 (3) (2010) 607–615.
[200] E. Badogiannis et al., Metakaolin as a main cement constituent. Exploitation of poor Greek kaolins, Cem. Concr. Compos. 27 (2) (2005) 197–203.
[201] G. Görhan, R. Aslaner, O. Şinik, The effect of curing on the properties of metakaolin and fly ash-based geopolymer paste, Compos. B Eng. 97 (2016) 329–335.
[202] P. Chindaprasirt et al., Effect of SiO 2 and Al 2 O 3 on the setting and hardening of high calcium fly ash-based geopolymer systems, J. Mater. Sci. 47 (12) (2012) 4876–4883.
[203] D. Adak, M. Sarkar, S. Mandal, Effect of nano-silica on strength and durability of fly ash based geopolymer mortar, Constr. Build. Mater. 70 (2014) 453–459.
[204] H.Y. Zhang et al., Thermal behavior and mechanical properties of geopolymer mortar after exposure to elevated temperatures, Constr. Build. Mater. 109 (2016) 17–24.
[205] P.N. Lemougna et al., Influence of the chemical and mineralogical composition on the reactivity of volcanic ashes during alkali activation, Ceram. Int. 40 (1) (2014) 811–820.
[206] J.N.Y. Djobo et al., Reactivity of volcanic ash in alkaline medium, microstructural and strength characteristics of resulting geopolymers under different synthesis conditions, J. Mater. Sci. 51 (22) (2016) 10301–10317.
[207] E.N. Kani, A. Allahverdi, Investigating shrinkage changes of natural pozzolan based geopolymer cement paste, Iran J. Mater. Sci. Eng. 8 (3) (2011) 50–60.
[208] J.N.Y. Djobo et al., Mechanical activation of volcanic ash for geopolymer synthesis: effect on reaction kinetics, gel characteristics, physical and mechanical properties, RSC Adv. 6 (45) (2016) 39106–39117.
[209] W. Wu et al., Influence of admixtures on rheological properties and heat of hydration of alkali aluminosilicate cement, Adv. Cem. Res. 29 (9) (2017) 397–403.
[210] F. Xie et al., Reaction kinetics and kinetics models of alkali activated phosphorus slag, Constr. Build. Mater. 237 (2020) 117728.
[211] X. Gao et al., Investigation on a green olivine nano-silica source based activator in alkali activated slag-fly ash blends: reaction kinetics, gel structure and carbon footprint, Cem. Concr. Res. 100 (2017) 129–139.
[212] D. Krizan, B. Zivanovic, Effects of dosage and modulus of water glass on early hydration of alkali–slag cements, Cem. Concr. Res. 32 (8) (2002) 1181–1188.
[213] C. Shi, R.L. Day, A calorimetric study of early hydration of alkali-slag cements, Cem. Concr. Res. 25 (6) (1995) 1333–1346.
[214] D.E. Angulo-Ramírez, R.M. de Gutiérrez, F. Puertas, Alkali-activated Portland blast-furnace slag cement: Mechanical properties and hydration, Constr. Build. Mater. 140 (2017) 119–128.
[215] Shearer, C.R., et al., The early age behavior of biomass fired and co-fired fly ash in concrete. Proceedings of World of Coal Ash, Denver, CO, 2011.
[216] D. Ravikumar, N. Neithalath, Reaction kinetics in sodium silicate powder and liquid activated slag binders evaluated using isothermal calorimetry, Thermochim. Acta 546 (2012) 32–43.
[217] B.S. Gebregziabiher, R. Thomas, S. Peethamparan, Very early-age reaction kinetics and microstructural development in alkali-activated slag, Cem. Concr. Compos. 55 (2015) 91–102.
[218] W.-H. Yang et al., A study of the effect of light-burnt dolomite on the hydration of alkali-activated Portland blast-furnace slag cement, Constr. Build. Mater. 57 (2014) 24–29.
[219] B. Yuan, Q. Yu, H. Brouwers, Reaction kinetics, reaction products and compressive strength of ternary activators activated slag designed by Taguchi method, Mater. Des. 86 (2015) 878–886.
[220] S.-D. Wang, K.L. Scrivener, Hydration products of alkali activated slag cement, Cem. Concr. Res. 25 (3) (1995) 561–571.
[221] K.L. Scrivener, A. Nonat, Hydration of cementitious materials, present and future, Cem. Concr. Res. 41 (7) (2011) 651–665.

[222] S. Chithiraputhiran, N. Neithalath, Isothermal reaction kinetics and temperature dependence of alkali activation of slag, fly ash and their blends, Constr. Build. Mater. 45 (2013) 233–242.
[223] C.R. Shearer, K.E. Kurtis, Use of biomass and co-fired fly ash in concrete, ACI Mater. J. 112 (2) (2015) 209–218.
[224] A. Brough, A. Atkinson, Sodium silicate-based, alkali-activated slag mortars: part I. Strength, hydration and microstructure, Cem. Concr. Res. 32 (6) (2002) 865–879.
[225] A. Brough et al., Sodium silicate-based alkali-activated slag mortars: Part II. The retarding effect of additions of sodium chloride or malic acid, Cem. Concr. Res. 30 (9) (2000) 1375–1379.
[226] S. Song, H.M. Jennings, Pore solution chemistry of alkali-activated ground granulated blast-furnace slag, Cem. Concr. Res. 29 (2) (1999) 159–170.
[227] D. Rothstein et al., Solubility behavior of Ca-, S-, Al-, and Si-bearing solid phases in Portland cement pore solutions as a function of hydration time, Cem. Concr. Res. 32 (10) (2002) 1663–1671.
[228] T.A. Saleh, V.K. Gupta, Synthesis and characterization of alumina nano-particles polyamide membrane with enhanced flux rejection performance, Sep. Purif. Technol. 89 (2012) 245–251.
[229] B. Almuhsin, T. al-Attar, Q. Hasan, Effect of discontinuous curing and ambient temperature on the compressive strength development of fly ash based Geopolymer concrete, MATEC Web Conf. 162 (2018) 02026.